ISSN 0869-5938, Stratigraphy and Geological Correlation, 2014, Vol. 22, No. 1, pp. 61–95. © Pleiades Publishing, Ltd., 2014.
Original Russian Text © E.A. Shcherbinina, G.N. Aleksandrova, A.I. Iakovleva, S.I. Stupin, E.Yu. Zakrevskaya, 2014, published in Stratigrafiya. Geologicheskaya Korrelyatsiya, 2014, Vol. 22, No. 1, pp. 65–99.

Microbiota and Stratigraphy of Lower Paleogene Deposits of the Urma Plateau, Central Dagestan

E. A. Shcherbinina[a], G. N. Aleksandrova[a], A. I. Iakovleva[a], S. I. Stupin[a], and E. Yu. Zakrevskaya[b]

[a]*Geological Institute of the Russian Academy of Sciences, Pyzhevskii per. 7, Moscow, 119017 Russia*
e-mail: katuniash@gmail.com
[b]*Vernadsky State Geological Museum, Mokhovaya ul. 11, Moscow, 125009 Russia*

Received September 5, 2011; in final form, November 6, 2012

Abstract—The study of nannofossils, dinocysts, and foraminifera from Paleogene deposits of the Urma Plateau of Central Dagestan revealed the Paleocene–Eocene age of the Gray Formation, to apply zonations based on of all three groups of microplankton, and to correlate the regional dinocyst and planktonic foraminifer zonations to the standard nannofossil scale. Nannofossil zonation of O. Varol's (1989) is shown to be successfully applied for subdivision of Danian deposits. The large foraminifer assemblage found in the lower Eocene deposits is correlated to the NP12–NP13 zones of the nannofossil scale.

Keywords: Paleocene, Eocene, nannofossils, dinocysts, foraminifera, zonal stratigraphy, eastern Caucasus

DOI: 10.1134/S0869593814010055

INTRODUCTION

The basin of the northeastern Caucasus, Dagestan, represented relatively deep part of the NE Peri-Tethys. This is very interesting geologically area, where perfect exposition, completeness and weak diagenesis of the lower Paleogene marine carbonate deposits can provide successful detailed stratigraphic works based on study of different groups of fossil microorganisms. A broad belt of the Paleogene deposits extends NW-SE across Dagestan, forming northeastern foothill of the Greater Caucasus. Danian deposits are represented by compact gray clayey and sandy-clayey limestones with individual intercalations of marls and siliceous rocks. The overlying soft sandy marls are incorporated in so-called Foraminiferal Formation, which changes its thickness from 10–20 to 350–360 m throughout the territory of Dagestan (Galin et al., 1963). The deposits of this formation vary greatly in color, that enable to identify the "Gray" Formation in the south of Dagestan and the "Variegated" Formation in the northern submontane part of Dagestan.

The deposits of the Variegated Formation were studied in detail by Shatsky (1963) in several outcrops throughout the area of their distribution. Later, these formations were shown to be co-eval (Golubyatnikov, 1938, 1940; Shutskaya and Kuznetsova, 1953; Mikulenko, 1962). The deposits of the "Gray" Formation grades into variegated deposits at the latitude of the village of Gubden, Central Dagestan. The Urma Plateau is an individual structure in the central Dagestan formed by large syncline with the gray-colored Paleogene deposits in the core (Fig. 1).

The stratigraphic scheme of Paleogene deposits of Dagestan is poorly developed. For a long time, "Gray" and "Variegated" Formations were considered as Paleocene–Eocene. As a result of detailed study of the sections along Sunzha and Khalagork rivers made by Shutskaya (1970), they were subdivided using zonal Crimea–Caucasus stratigraphic scheme based on planktonic foraminifera and correlated to deposits of the Central Caucasus. The study of nannofossils in the section along the Rubas-Chai River, Southern Dagestan, enabled the zonal subdivision based on the standard nannofossil zonation and estimation of the volume of stratigraphic hiatuses (N.G. Muzylev, unpublished data).

We made an integrated study of nannofossil, small and large foraminiferal and dinocyst assemblages in the Ostrich Farm section, situated in the southeastern margin of the Urma plateau near the Levashi village, to determine exact stratigraphic range of deposits of this area for the first time and to correlate zonal subdivisions based on three microplankton groups.[1]

[1] The section was named in 2003 after the ostrich farm located near the base of the outcrop of siliceous deposits at the Makhachkala–Levashi highway.

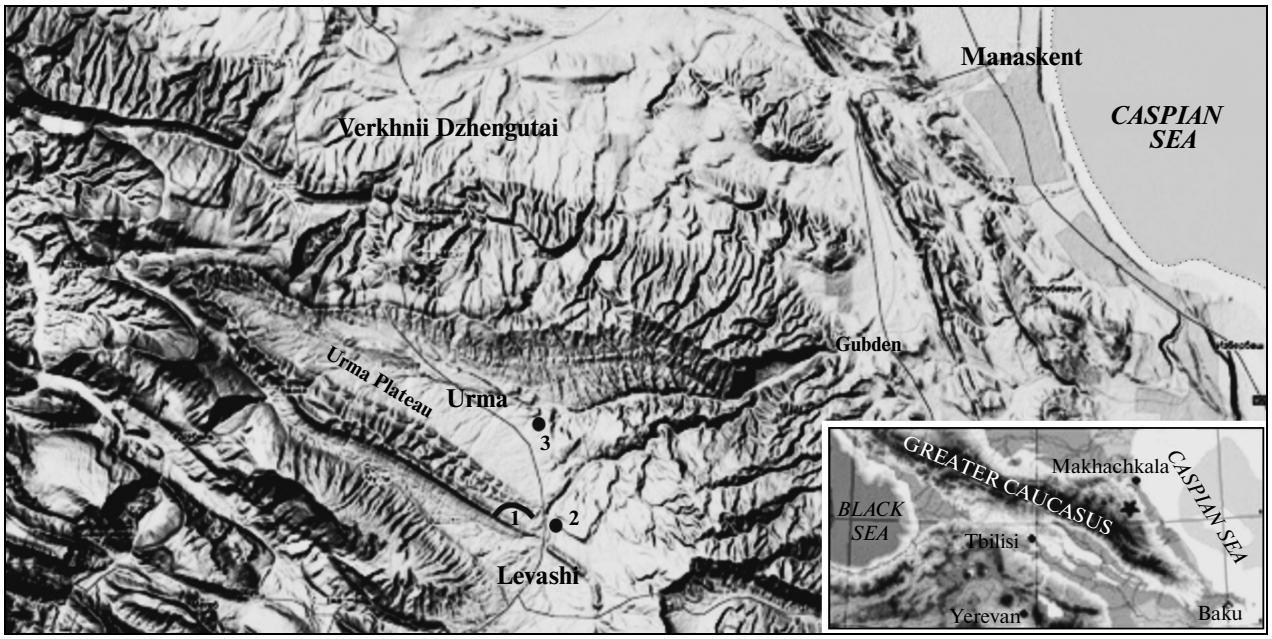

Fig. 1. Geographic position of the Ostrich Farm section in the Caucasus (insert) and the Urma Plateau, Central Dagestan. (1) Location of a series of outcrops of Paleocene–early Eocene deposits; (2) outcrop of Lutetian siliceous deposits; (3) outcrop of the upper Lutetian–lower Bartonian marl deposits.

MATERIALS AND METHODS

Paleogene deposits were described and sampled in a series of outcrops along an unnamed stream entering the Khalagork River in the northern outskirts of the village of Levashi (42°16′12″ N, 47°21′19″ E). This work is based on the study of more than 100 samples collected from the accessible part of the Ostrich Farm section starting from the upper Danian deposits and provided parallel examination of nannofossils, dinocysts, and foraminifers.

Nannofossils were studied from all samples, prepared using the standard procedure (Bown, 1998). The study was performed using an Olympus BX-41 microscope with an Infinity X video adapter. Smear-slides are stored in the Laboratory of Micropaleontology of the Geological Institute (GIN RAS, Moscow).

The treatment of the palynological samples was carried out by the method developed at GIN RAS. The technique of sample preparation was as follows: (1) dissolution of carbonates with 10% HCl; (2) treatment of samples with 5% Na_2HPO_4OH and elutriation of clay minerals; (3) separation of the remaining sludge by centrifugation in heavy liquid with a density of 2.25 g/cm^3 [3] (solution of KI and CdI) to extract palynomorphs; (4) pouring the treated material into test tubes with glycerin for further study and storage. The studied samples and smear-slides are stored in the Laboratory of Paleofloristics (GIN RAS, Moscow). The smear-slides were studied using an Axiostar plus microscope. For palynological analysis, quantitative evaluation of the composition of phytoplankton assemblages (at least 200 representatives per sample) was made and after that, smear-slides were examined again to find rare taxa.

To study foraminifers, the samples were washed through a 70 μm sieve according to the standard procedure and studied using an MBS-1 microscope.

PALEOGENE DEPOSITS OF THE URMA PLATEAU

Danian deposits of the Urma Plateau are composed of compact thick-bedded limestones with individual intercalations of laminated soft marls (Fig. 2a). These limestones are exposed as a nearly 45° dipping ridge, bounding the southern edge of the plateau. The bedding is periodically disturbed by submarine slumping folds. In the upper part of the Danian sequence, limestones become silty, intercalations of laminated marls become more frequent and their thickness increases (to 0.5–0.7 m); numerous remains of echinoids and rare siliceous nodules appear. The total thickness of the studied part of the sequence is ~50 m, where 13 m interval disturbed by submarine slumping is missed from sampling.

The rough boundary ("hard-ground") of Danian gray limestone is overlain by thin-bedded silty marls (Fig. 2b). Upsection, the marls become rather homo-

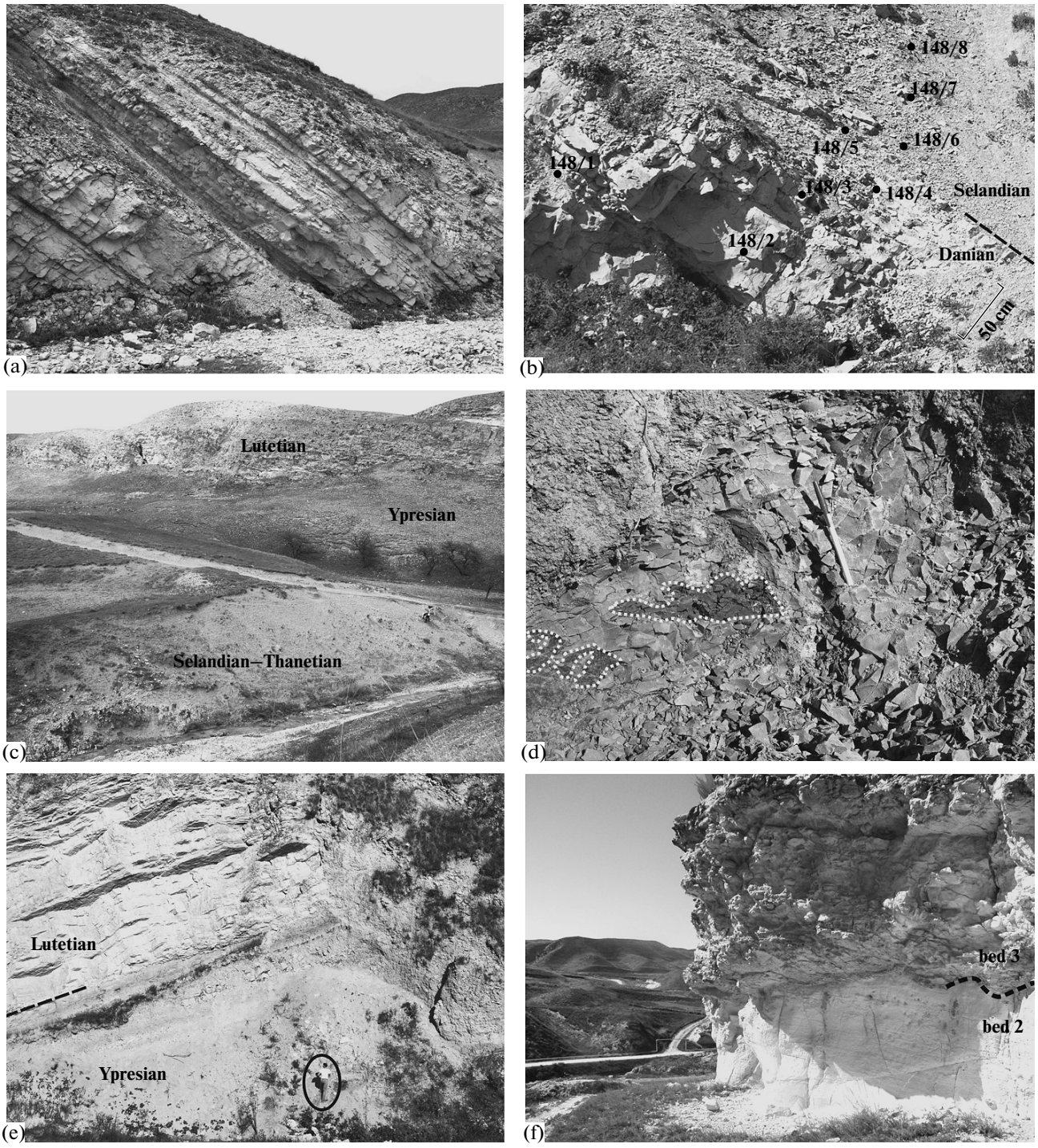

Fig. 2. Deposition of different Paleogene strata in the Ostrich Farm section: (a) Upper Danian deposits; (b) Danian–Selandian boundary and the scheme of sampling; (c) relationship between Selandian–Thanetian, Ypresian, and Lutetian deposits in outcrops along the unnamed stream (photo by Yu.O. Gavrilov); (d) sapropelite lens at the Paleocene/Eocene transition; (e) upper part of the marl sequence and spongolites in the outcrop along the unnamed stream (photo by Yu.O. Gavrilov); (f) spongolite-siliceous marl contact zone in the outcrop along the Makhachkala–Levashi road (Urma Plateau) (point 2 in Fig. 1).

geneous, soft, greenish gray, and contain lower silty compound. Gradually, the marls become more compact and thick-bedded, probably, due to an increase of calcium carbonate content (Fig. 2c). The thickness of this unit up to the top of the outcrop (on the left bank of the stream) is about 35 m. Upsection, after ~7 m of an unexposed part, the sampling was carried out in a series of outcrops of similar marl along both sides of the stream.

In total, the stratum of nearly 33 m in thickness was sampled up to the level of occurrence of isomorphous inclusions of sapropel-like clayey material and lenses of paler carbonate rocks. This level likely corresponds to a hiatus in sedimentation and redeposition of blocks of weakly lithified deposits. It is likely that this level corresponds to the timing of underwater slumping of sediments. The occurrence of fragments of sapropelite deposits (Fig. 2e) points to primary deposition of TOC-rich sediment which evidently corresponds to sapropelitic bed spreading throughout the northeastern Peri-Tethys, from Crimea to Central Asia, and related to the global paleoenvironmental crisis known as the Paleocene–Eocene Thermal Maximum (PETM) (Gavrilov et al., 2003; Aleksandrova and Shcherbinina, 2011). Upward, the sedimentation regime changes and the upper 5 m part of the marl unit shows signs of frequent short stratigraphic hiatuses corresponding to thin sandy intercalations containing small pebbles and broken shells. In the uppermost part of the section, two distinct beds (5 and 10 cm) of compact red sandstones occur.

Upsection, siliceous deposits of highly variable laterally thickness onlap the unevenly eroding boundary (Fig. 2e). In the studied outcrop in the left side of the stream, siliceous rocks are represented by 15 m thick homogenous white spongolite with conglomerates at the base. Westward, this stratum wedges out at a short distance and eastward its thickness significantly reduces. However, in an outcrop situated approximately 500 m downstream at the point where the stream is crossed by the Makhachkala–Levashi road (point 2 in Fig. 1), the siliceous sequence is as follows (Fig. 2f):

1. At the base of siliceous deposits, ~12 m thick massive nodular brownish gray siliceous limestone overlies greenish gray marl. The nannofossil study showed late Paleocene age (NP9 zone) for this stratum and thus, Ypresian sediments appeared to be eroded in this locality.

2. Soft white spongolites with rare nodules of gray flint, similar to those occurring in the above-described outcrop along the stream. Thickness is 7.5 m.

3. Friable siliceous marl ~8 m thick onlap the rough boundary with deep erosional pockets.

4. Pale gray silty siliceous limestones, ~9 m of visible thickness.

Similar pale gray limestone are exposed in a small ~2.5 m thick exposure located ~200 m northward and few meters above, at the top of Urma Plateau.

In another outcrop (point 3 in Fig. 1) exposed in the central part of the plateau approximately 3 km northward of the above-described section, the alternation of compact pale gray limestones and thin-bedded pale gray marls (visible thickness is about 3 m) is exposed. This unit is armored by a bed of compact siliceous limestones, distinctly visible even in unexposed areas and used as a marker horizon. Upsection, thin-bedded soft pale gray marls of 1.5 m of observed thickness lies.

During several field seasons, marl deposits were sampled in detail; Danian limestones and siliceous sequence were sampled with lower resolution.

RESULTS

Nannofossils

Calcareous nannofossils are presented across the most part of section studied with the exception for the basal stratum of siliceous sequence, although they show significant variations in abundance, species diversity, and preservation in different stratigraphic intervals. The nannofossil assemblage of the Danian compact limestones is rather poor and characterized by moderate to poor preservation. The nannofossil abundance increases gradually toward the top of the Danian deposits and remains relatively high up to siliceous sequence (Tables 1–3), where the main biogenic component becomes presented by siliceous sponge spicules, while dinocysts and foraminifera are absent. The most ancient nannofossil assemblage (samples 140, 141; Fig. 3) contains *Prinsius martinii*, *P. dimorphosus*, *Coccolithus pelagicus*, *C. robustus*, *Neochiastozygus modestus*, *Placozygus sigmoides*, *Chiasmolithus danicus*, *Cruciplacolithus primus*, *C. subrotundus*, and *Toweius* sp.; *Braarudosphaera bigelowii*, *B. discula*, micrantoliths, and calcite dinocysts *Thoracosphaera* spp. are common. The absence of *Neochiastozygus eosaepes*, whose disappearance marks the upper boundary of the NTp6 zone, allows us to attribute this assemblage to the NTp7A subzone of Varol zonation (Varol, 1989).

The marker species of the late Danian NP4 zone of Martini (1971) standard zonation, *Ellipsolithus macellus* (Martini, 1971) was not found in this interval. Immediately above the 13 m interval disturbed by submarine slumping, the first occurrence (FO) of *Chiasmolithus edentulus*, marking the bottom of the NTp7B subzone, is detected. At the same level, the FO of common *Lithoptychius* cf. *chowii* is found. The first occurrence of numerous *Sphenolithus primus*, which

Table 1. Distribution of nannoplankton species in Danian–Thanetian deposits (Ostrich Farm section)

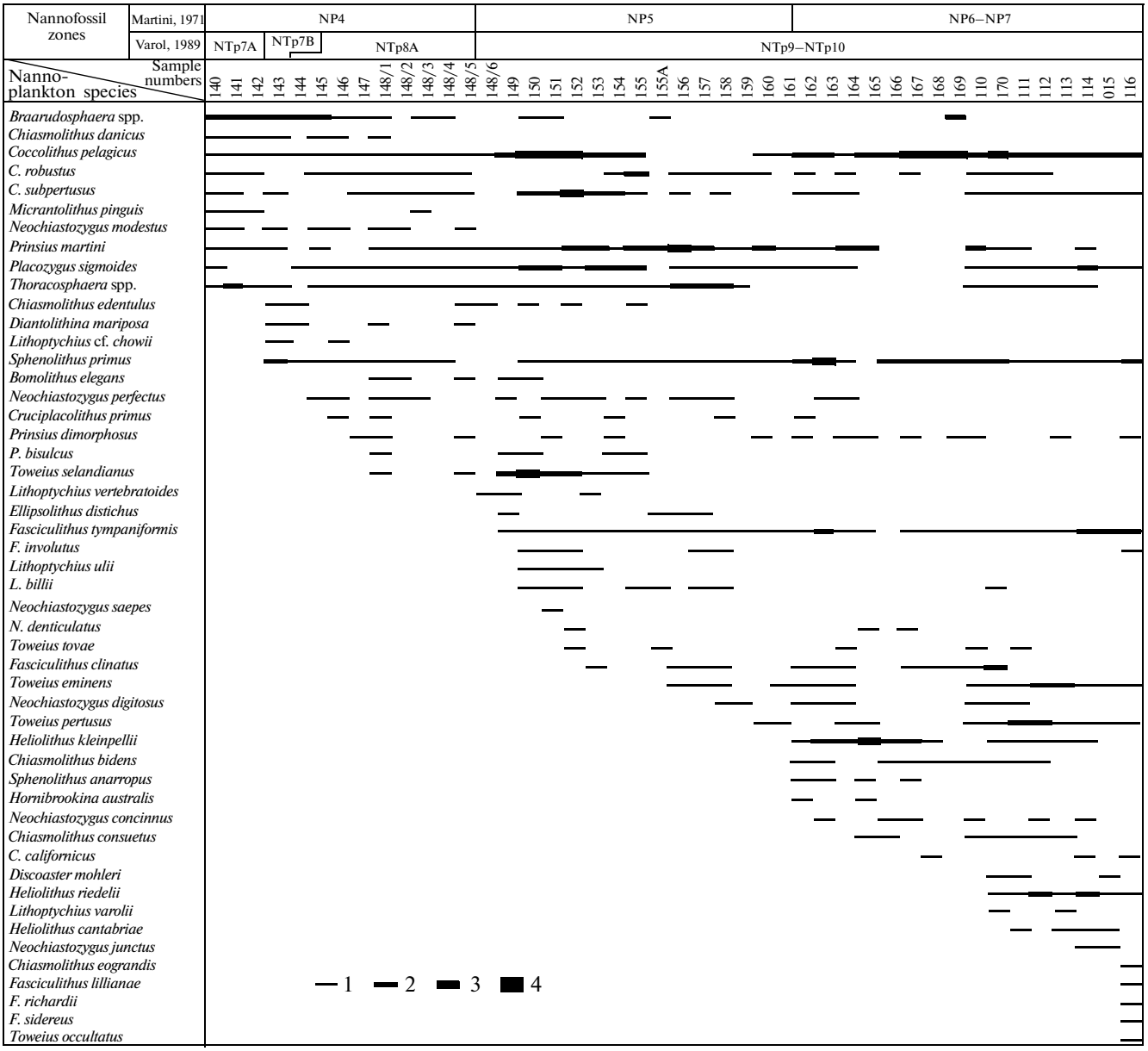

Nannofossil abundance here and Tables 2, 3: (1) few (several specimens in smear-slide); (2) rare (several specimens in the row); (3) common (up to 1–2 specimens in a field of view); (4) abundant (>3 specimens in a field of view).

marks the bottom of the NTp8 zone, coincides with the FOs of *Bomolithus elegans*, *Toweius* sp., and large *Prinsius martini*. Nannofossil assemblage of this interval becomes more abundant and diverse (Plate I) and contains rather common redeposited Cretaceous species. The upper 5 m thick interval of Danian deposits is characterized by a decrease in nannofossil abundance; the reduction of pentalithes (*Braarudosphaera* and *Micrantolithus*) and domination of *Toweius* spp. over *Coccolithus* spp. are noted. The simultaneous FOs of *Lithoptichius ulii* and *F. janii*, marking the bases of terminal Danian NTp8B and NTp8C, respectively, as well as the FO of *F. tympaniformis*, marking the base of Selandian NP5 zone, were found immediately above the erosional surface, which cut the top of Danian deposits. This evidences the stratigraphic hiatus at the Danian/Selandian boundary ranging NTp8B–NTp8C subzones.

The overlying sequence of soft monotonous marls is characterized by abundant and diverse nannofossil assemblage showing rapid diversification of *Toweius*, *Fasciculithus*, and *Neochiastozigus* spp. (Fig. 3). This community contains a lot of evidently unknown species or species described in the uncertain definition

Table 2. Distribution of nannofossils in Thanetian–Ypresian deposits in the Ostrich Farm section

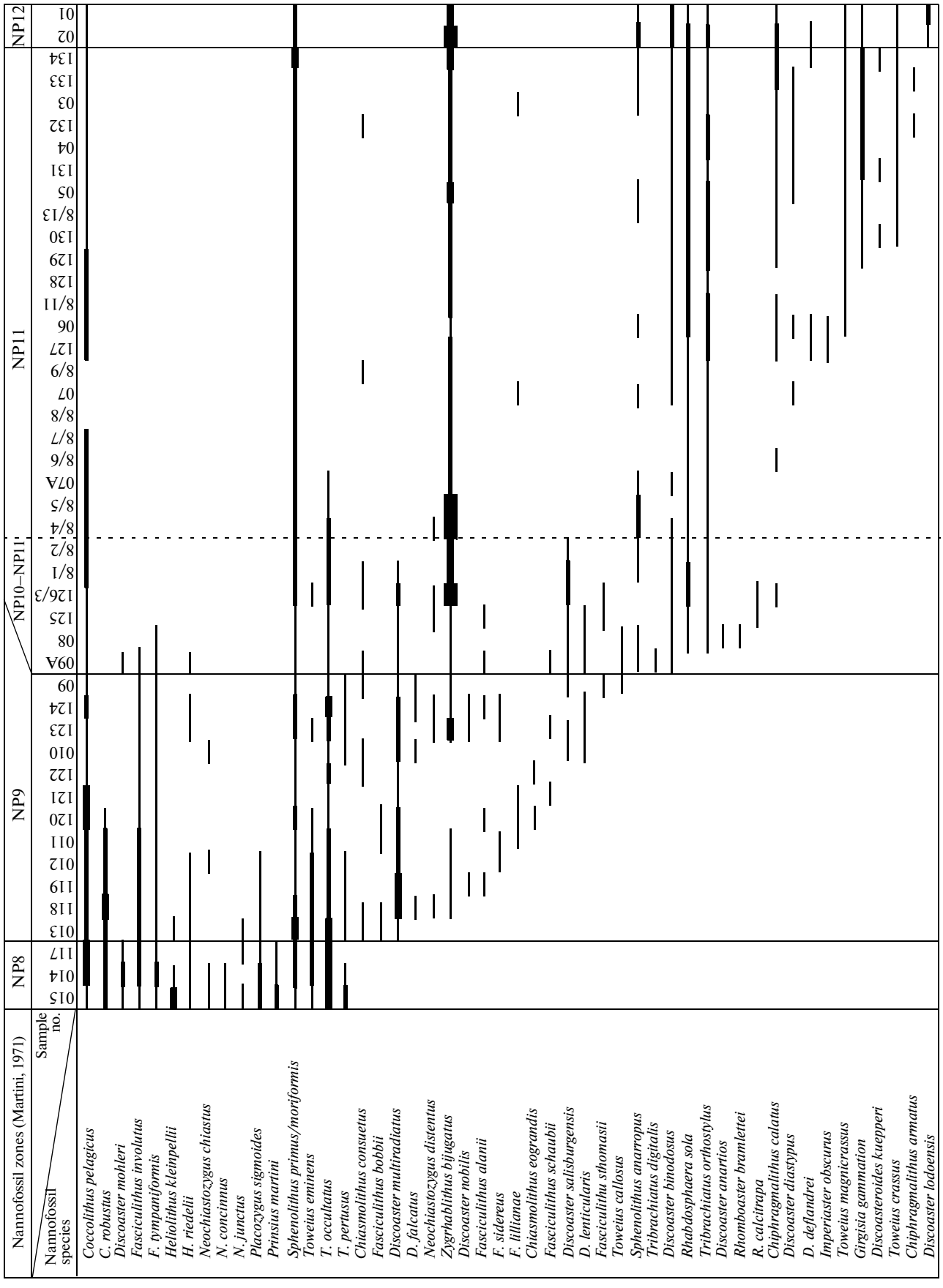

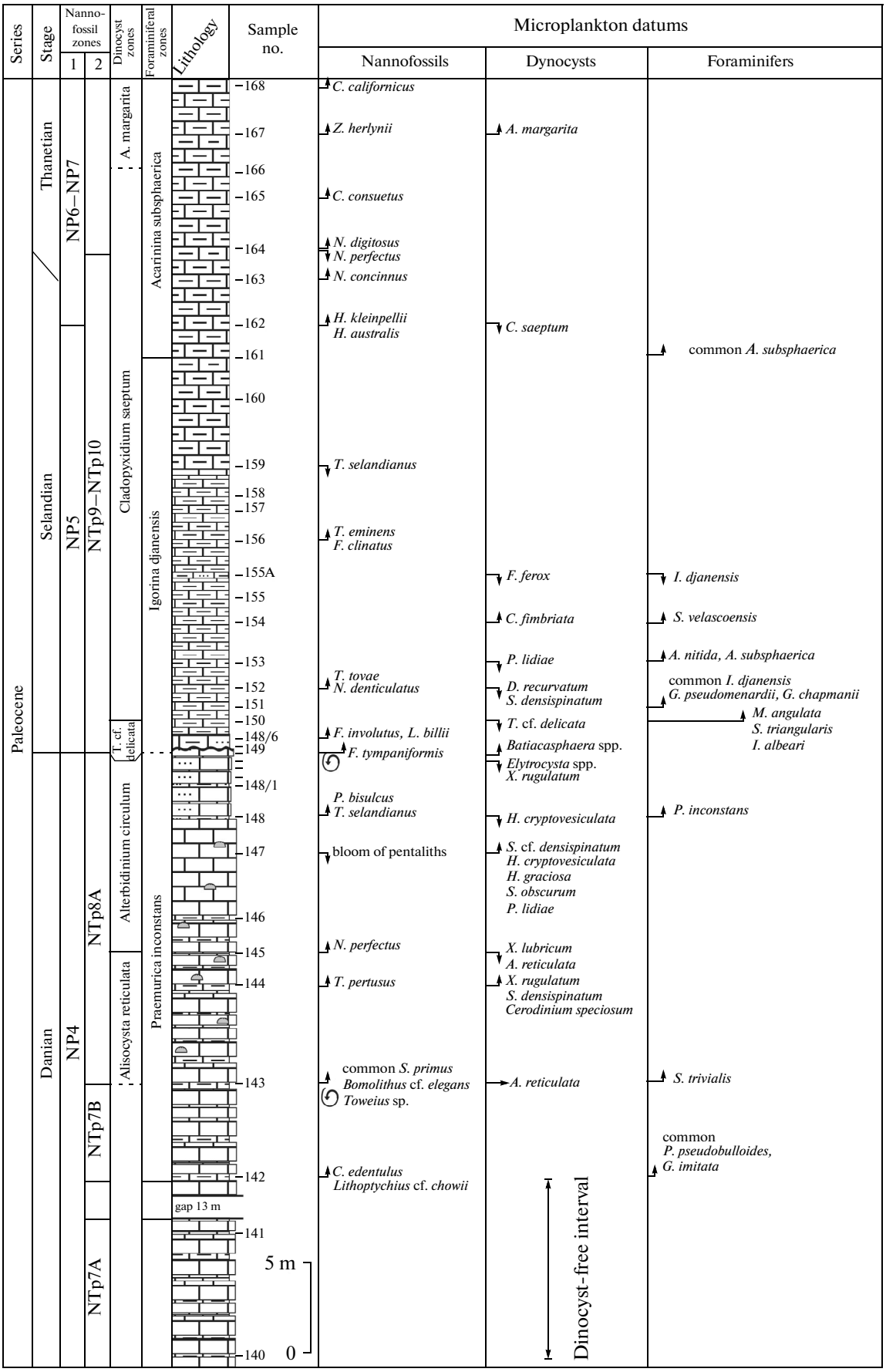

Fig. 3. Zonal subdivision and the levels of the first and last occurrences of microplankton species in Danian–lower Thanetian deposits (Ostrich Farm section). (1) Martini's zonation (Martini, 1971), (2) Varol's zonation (Varol, 1989). Legend is given in Fig. 4.

Table 3. Distribution of nannofossil species in the middle Eocene deposits (Ostrich Farm section)

Nannofossil zones	Okada and Bukry, 1980	CP15A	CP15B
	Martini, 1971	NP15–NP16	
Nannofossil species \ Sample no.		11/04 10/04 9/04 8/04 7/04 6/04 5/04 4/04 3/04 2/04 1/04 5/08 6/08 7/08 8/08 1/08 2/08 3/08	
Braarudosphaera bigelowii		— — — — — — — — — — — — — — — — — —	
Coccolithus formosus		— — — — — — — — — — — — — — — — — —	
C. pelagicus		— — — — — — — — — — — — — — — — — —	
Discoaster binodosus		— — — — — — — — — — — — — — — — — —	
D. wemmelensis		— — — — — — — — — — — — — — — — — —	
Neococcolites dubius		— — — — — — — — — — — — — — — — — —	
Sphenolithus moriformis		— — — — — — — — — — — — — — — — — —	
S. obtusus		— — — — — — — — — — — — — — — — — —	
Triquetrorhabdulus inversus		— — — — — — — — — — — — — — — — — —	
Chiasmolithus grandis		— — — — — — — — — — — — — — — — — —	
Discoaster barbadiensis		— — — — — — — — — — — — — — — — — —	
D. saipanensis		— — — — — — — — — — — — — — — — — —	
Sphenolithus radians		— — — — — — — — — — — — — — — — — —	
Zygrhablithus bijugatus		— — — — — — — — — — — — — — — — — —	
Coronocyclus nitescens		— — — — — — — — — — — — — — — — — —	
Chiasmolithus gigas		— — — — — — — — — — — — — — — — — —	
Reticulofenestra umbilicus		— — — — — — — — — — — — — — — — — —	
Sphenolithus spiniger		— — — — — — — — — — — — — — — — — —	
Chiasmolithus nitidus		— — — — — — — — — — — — — — — — — —	
Cyclicargolithus floridanus		— — — — — — — — — — — — — — — — — —	
Discoaster deflandrei		— — — — — — — — — — — — — — — — — —	
Lanternites duocavus		— — — — — — — — — — — — — — — — — —	
Reticulofenestra dictyoda		— — — — — — — — — — — — — — — — — —	
Discoaster nonaradiatus		— — — — — — — — — — — — — — — — — —	
Dictyococcites bisectus		— — — — — — — — — — — — — — — — — —	
Reticulofenestra hillae		— — — — — — — — — — — — — — — — — —	

(Plate III). The earliest assemblage of Selandian interval, referring to the NP5 zone, is still rather poor and besides the FO of *Fasciculithus tympaniformis*, it is marked by FO of *Toweius eminens*, which became a common element of the late Paleocene nannoflora. This is the highest level where it is still possible to use Varol's zonation developed for detailed biostratigraphy of the Paleogene deposits of the North Sea (Varol, 1989). The FO of *Heliolithus kleinpellii* marks the base of the NP6 zone ~25.5 m above the Danian–Selandian boundary. Above this level, a significant increase of nannofossil species diversity began owing to the occurrence of new species of genera *Neochiastozygus* and *Chiasmolithus*.

The range of NP7 zone can not be identified in the Ostrich Farm section since the marker species of its base *Discoaster mohleri* first appear at the level of the FO of the marker species of NP8 zone *Heliolithus riedelii*, although there is no erosional signs in this interval. This suggests that *D. mohleri* appeared in this basin later than its evolutionary FO. At the upper part of this undivided Thanetian interval, a 3rd radiation of fasciculiths began, during which *Fasciculithus junctus*, *F. lillianae*, *F. alanii*, *F. sidereus*, *F. schaubii*, a.o., successively appear. The zone NP9, identified by the appearance of *Discoaster multiradiatus* (Fig. 4), marks the stage of further increase in nannofossil species diversity.

The Paleocene/Eocene transition is chatacterized by very intricated picture: younger species *Tribrachiatus digitalis*, *T. orthostylus* (sample 09A) marking the bases of NP10c and NP11 subzones, respectively, occur at the lower levels of the section than typical for the PETM *Rhomboaster cuspis*, *R. bramlettei*, *Discoaster araneus*, which were found at the level with sapropelitic lenses, Sample 08. Obviously, the presence of the mixed nannofossil assemblage is a result of complex hydrodynamic processes in the basin at the Paleocene/Eocene boundary, which led to formation of a conglomerate-like mass made of fragments of weakly lithified rocks of similar composition, but of different age. The nannofossil assemblage of this interval (samples 08–8/2) includes taxa deposited in situ and redeposited Cretaceous and Early Paleocene species. The upper 6.5 m of sampled interval of the section comprises "normal" Ypresian nannofossil assem-

Fig. 4. Zonal subdivision and the levels of the first and last occurrence of microplankton species in the Thanetian–Ypresian deposits of the Ostrich Farm section. Abbreviations: *A. au.*—*Apectodinium augustum*, *M. a.*—*Morozovella acarinata*, *M. sub.*—*Morozovella subbotinae* s. str. subzone.

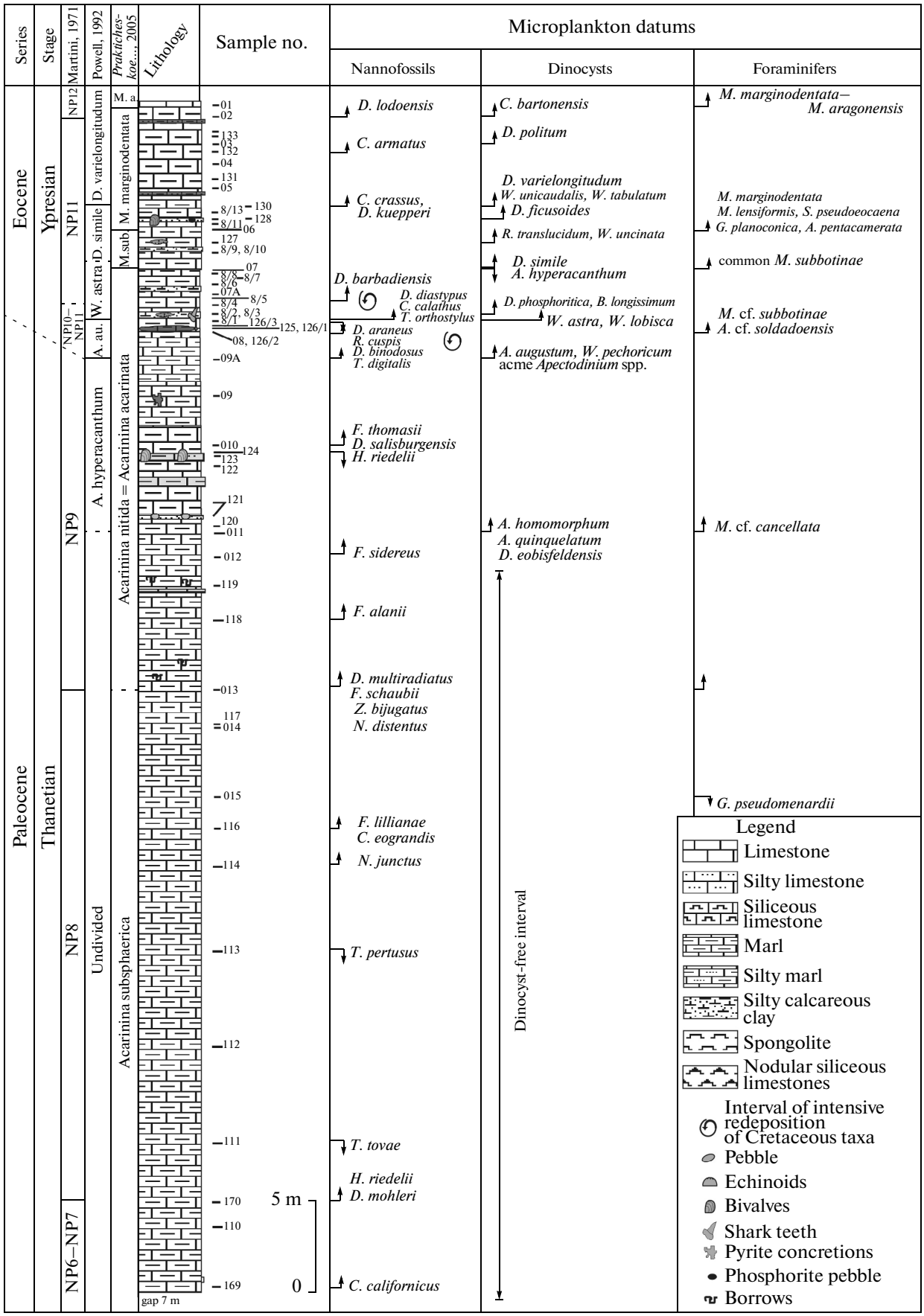
Series
Stage
Martini, 1971
Powell, 1992
Praktichesko..., 2005
Lithology
Sample no.
Microplankton datums
Nannofossils
Dinocysts
Foraminifers
Paleocene
Eocene
Thanetian
Ypresian
NP6–NP7
NP8
NP9
NP10–NP11
NP11
NP12
Undivided
A. hyperacanthum
A. au.
W. astra
D. simile
D. varielongitudum
M. sub
M. marginodentata
M. a.
Acarinina subsphaerica
Acarinina nitida = Acarinina acarinata
gap 7 m
5 m
0
D. lodoensis
C. armatus
C. crassus, D. kuepperi
D. barbadiensis
D. diastypus
C. calathus
T. orthostylus
D. araneus
R. cuspis
D. binodosus
T. digitalis
F. thomasii
D. salisburgensis
H. riedelii
F. sidereus
F. alanii
D. multiradiatus
F. schaubii
Z. bijugatus
N. distentus
F. lillianae
C. eograndis
N. junctus
T. pertusus
T. tovae
H. riedelii
D. mohleri
C. californicus
C. bartonensis
D. politum
D. varielongitudum
W. unicaudalis, W. tabulatum
D. ficusoides
R. translucidum, W. uncinata
D. simile
A. hyperacanthum
D. phosphoritica, B. longissimum
W. astra, W. lobisca
A. augustum, W. pechoricum
acme Apectodinium spp.
A. homomorphum
A. quinquelatum
D. eobisfeldensis
Dinocyst-free interval
M. marginodentata–
M. aragonensis
M. marginodentata
M. lensiformis, S. pseudoeocaena
G. planoconica, A. pentacamerata
common M. subbotinae
M. cf. subbotinae
A. cf. soldadoensis
M. cf. cancellata
G. pseudomenardii
Legend
Limestone
Silty limestone
Siliceous limestone
Marl
Silty marl
Silty calcareous clay
Spongolite
Nodular siliceous limestones
Interval of intensive redeposition of Cretaceous taxa
Pebble
Echinoids
Bivalves
Shark teeth
Pyrite concretions
Phosphorite pebble
Borrows

Plate I

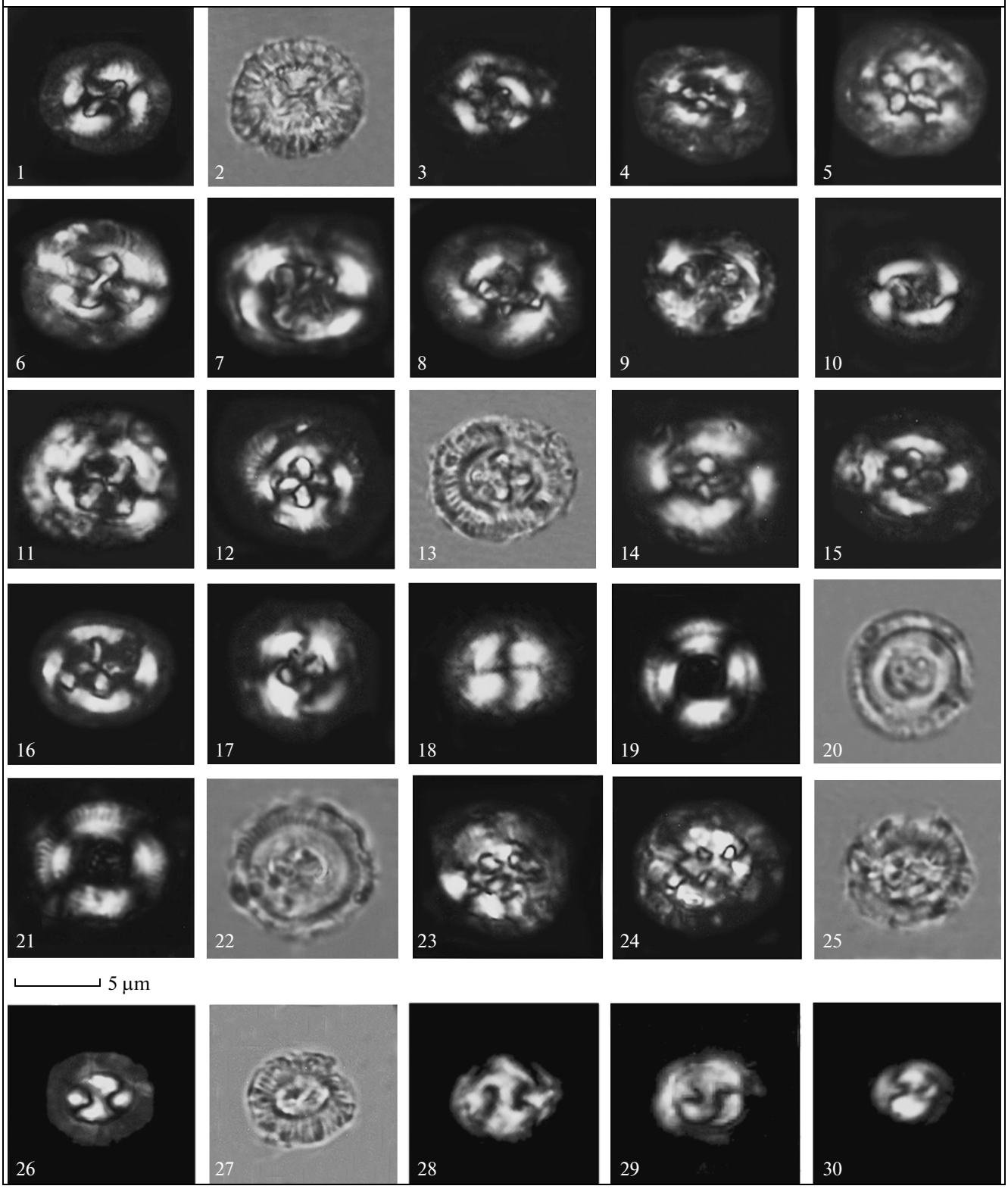
1
2
3
4
5
6
7
8
9
10
11
12
13
14
15
16
17
18
19
20
21
22
23
24
25
5 μm
26
27
28
29
30

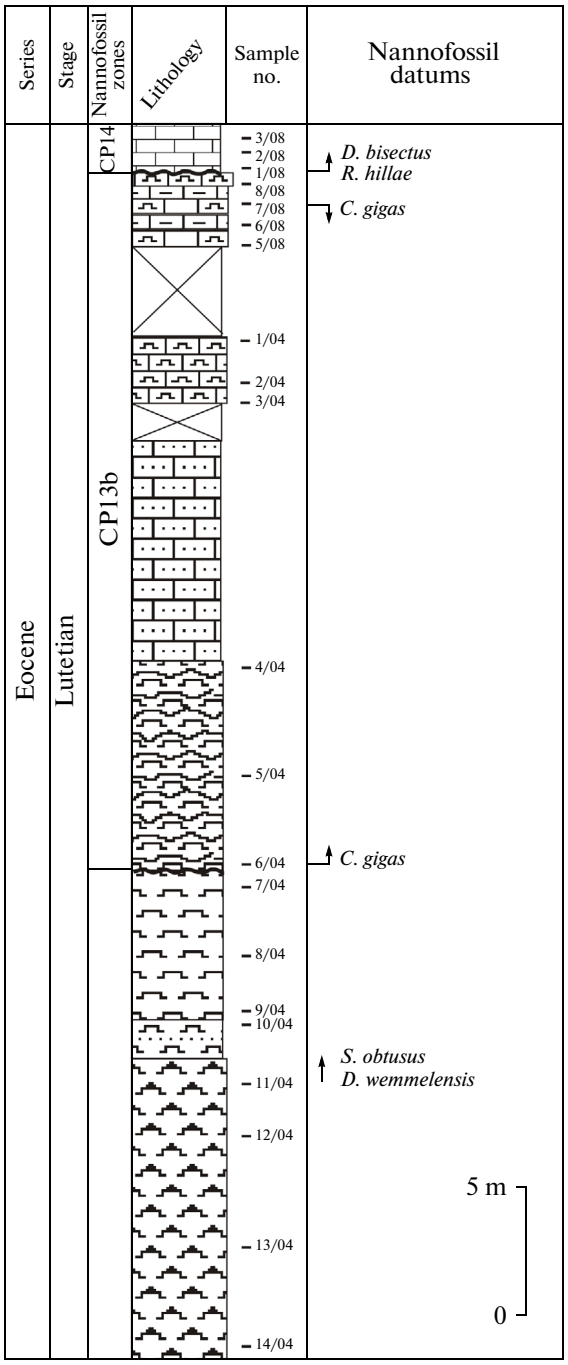

Fig. 5. Zonal subdivisions and levels of the FOs and LOs of nannofossil species in the middle Eocene deposits of Ostrich Farm section. For symbols see Fig. 4.

blage without significant redeposition. Below the top of the stratum (~0.8 m), the marker species of upper Ypresian NP12 zone *Discoaster lodoensis* appears.

The siliceous sequence contains abundant sponge spicules and fragments of radiolarians and diatoms, whereas the nannofossils become less diverse. The base of the lower unit of siliceous limestones is lack in nannofossils; they occur sporadically above the level of the Sample 11 (Fig. 5). Nannofossil assemblage of this interval is very poor and only the presence of *Sphenolithus obtusus* and *Discoaster wemmelensis* can be evidence of the Lutetian age of deposits. The occurrence of *Chiasmolithus gigas* at the base of siliceous marls indicates the Lutetian CP13b subzone, corresponding to the stratigraphic range of this species. Its presence in both small outcrops (2 and 3) up to the compact marker horizon suggests significant thickness of deposits accumulated during this time. At the uppermost sampled unit of pale marls, overlying the compact horizon, rather common nannofossils are found. *C. gigas* desappears in this interval and the co-occurrence of *Dictyiococcites bisectus* and *Reticulofenestra hillae* and *Chiasmolithus solitus* more likely indicates the CP14 zone.

Dinocysts

Dinocysts are not found in massive limestone at the base of the section (samples 140–142). They first occur from the upper more silty limestone (sample 143) in the middle of the NP4 and Praemurica inconstans zones (Table 4). Upsection (interval of samples of 143–145), the local zone Alisocysta reticulata was established. The upper boundary of this zone is fixed by the last occurrence (LO) of the index species. Dinocyst assemblage is dominated by *Spini-ferites* spp., *Achomosphaera ramulifera*, *A. alcicornu*, *Membranosphaera maastrichtica*, *Operculodinium*

Plate I. Light microscope images of the nannofossils of Ostrich Farm section. (1) *Chiasmolithus consuetus* (Bramlette et Sullivan) Hay et Mohler, sample 122, polarized light (PL); (2) the same specimen, normal light (OL); (3) *Chiasmolithus danicus* (Brotzen) Hay et Mohler, sample 141, PL; (4) *Cruciplacolithus asymmetricus* Van Heck et Prins, sample 144, PL; (5) *C. asymmetricus*, sample 143, PL; (6) *Cruciplacolithus edwardsii* Romein, sample 145, PL; (7) *Chiasmolithus bidens* Romein, sample 142, PL; (8) *Chiasmolithus inconspicuous* Van Heck et Prins, sample 144, PL; (9) *C. inconspicuous*, sample 143, PL; (10) *Chiasmolithus titus* Gartner, sample 118, PL; (11) *Chiasmolithus edentulus* Van Heck et Prins, sample 168, PL; (12) *Cruciplacolithus intermedius* Van Heck et Prins, sample 144, PL; (13) the same specimen, OL; (14) *Cruciplacolithus primus* Perch-Nielsen, sample 142, PL; (15) *Cruciplacolithus tenuis* (Stradner) Hay et Mohler, sample 140, PL; (16) *Cruciplacolithus intermedius* Van Heck et Prins, sample 144, PL; (17) *Cruciplacolithus subrotundus* Perch-Nielsen, sample 140, PL; (18) *Coccolithus pelagicus* (Wallich) Schiller, sample 142, PL; (19) *Coccolithus robustus* (Bramlette et Sullivan) (Wind et Wise), sample 148-3, PL; (20) the same specimen, OL; (21) *Coccolithus subpertusus* (Hay et Mohler) Wei et Pospichal, sample 149, PL; (22) the same specimen, OL; (23) *Coccolithus* sp. 1, sample 142, PL; (24) *Coccolithus* sp. 1, another specimen, sample 142, PL; (25) the same specimen, OL; (26) large *Prinsius martini* (Perch-Nielsen) Haq, sample 140, PL; (27) the same specimen, OL; (28) *P. bisulcus* (Stradner) Hay et Mohler, sample 110, PL; (29) *P. bisulcus*, sample 164, PL; (30) *Prinsius dimorphosus* Perch-Nielsen, sample 145, PL.

Plate II

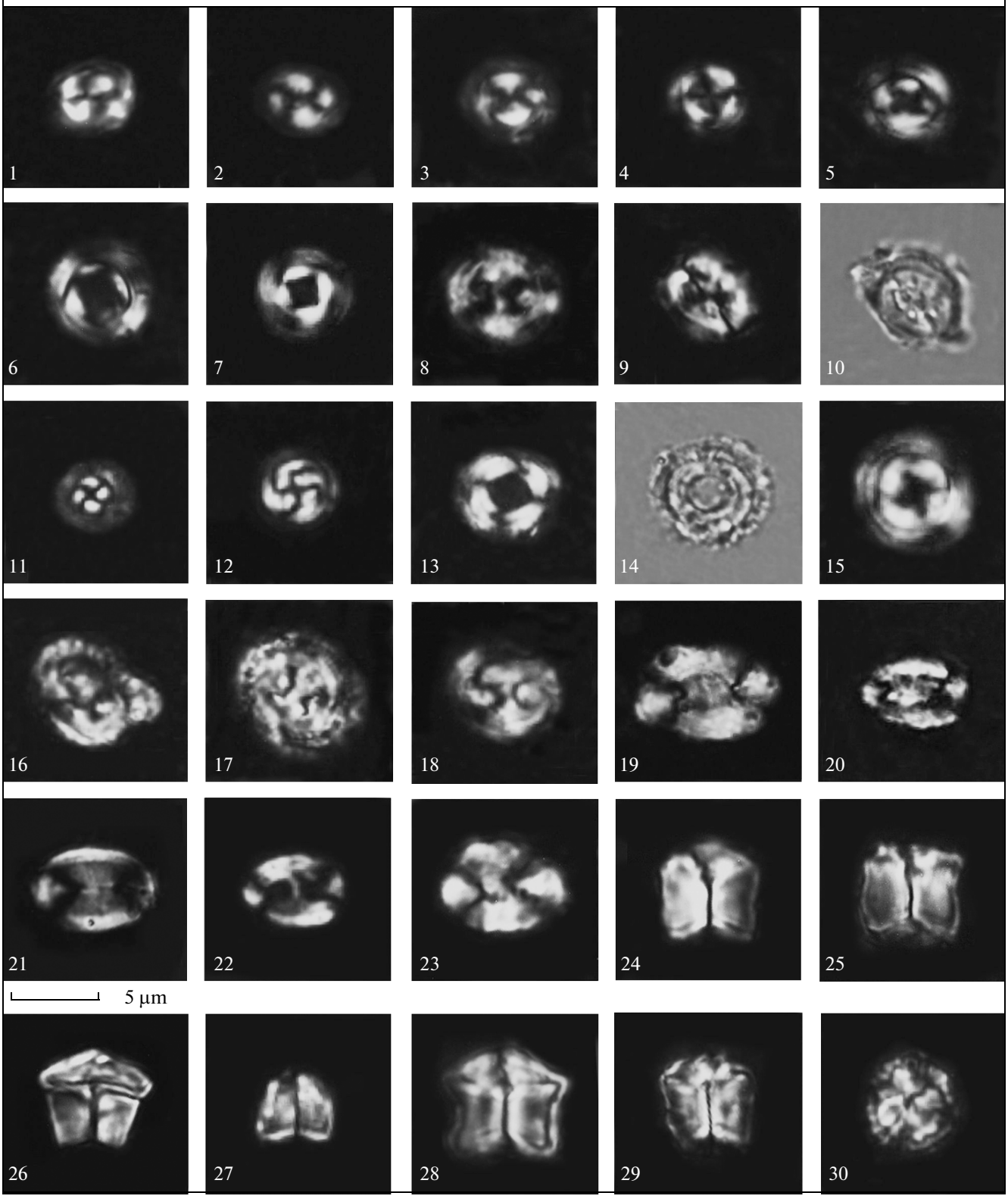
1
2
3
4
5
6
7
8
9
10
11
12
13
14
15
16
17
18
19
20
21
22
23
24
25
5 μm
26
27
28
29
30

microtrianum, *O. centrocarpum*, *Fibradinium annetorpense*, *Cordosphaeridium exilimurum*, *C. gracilis*, *Diphyes recurvatum*. Such species as *Alisocysta reticulata*, *Danea mutabilis*, *Xenicodinium lubricum*, *X. rugulatum*, *Hafniasphaera cryptovesiculata*, *Alterbidinium circulum*, *Areoligera coronata*, *Florentinia ferox*, *Kallosphaeridium yorubaense*, *Hystrichostrogylon coninkii*, *Hafniasphaera septata*, *Oligosphaeridium complex*, *Cladopyxidium saeptum*, *Hystrichosphaeridium tubiferum*, and *Elytrocysta* spp. are less common. The LOs of *Alisocysta reticulata* and *Xenicodinium lubricum* coincide with the FO of *Neochiastozygus perfectus* nannofossil. The LO of *Alisocysta reticulata* marks the top of the Alisocysta reticulata DP2a (Mudge and Bujak, 1996) subzone of the North Sea zonation and D2a subzone of the NW Europe zonation (Luterbacher et al., 2004).

In the overlying part of the section (Samples 145–149), the local Alterbidinium circulum zone was recognized; the upper boundary of the zone is marked by the LO of marker species. In the dinocyst assemblage of the upper part of the NP4 zone (the FO of *R. bisulcus*, *T. selandianus* nannofossils), the LO of *Hafniasphaera cryptovesiculata* was identified; in the uppermost part of the zone, the LOs of *X. rugulatum* and *Elytrocysta* spp. were detected. Co-occurrence of *Alterbidinium circulum* and *Spinidinium densispinatum* is typical of the Viborg 1 zone (Heilmann-Clausen, 1985, 1994), which nearly ranges the upper part of the NP4 zone and the lower part of the zone NP5 (Heilmann-Clausen, 1985). Besides, co-occurrence of these species is characteristic for the Spinidinium densispinatum zone (Powell, 1992). The Alterbidinium circulum zone was also identified in the Ivdel Formation of the northern Urals (Vasilyeva, 1999), the Talitsa Horizon of the Central Trans-Urals (Amon et al., 2003), and the Tsyganov Formation of the Peri-Caspian Region (Vasilyeva and Musatov, 2008).

The local Thalassiphora cf. delicata zone is in the upper part of NP5 zone (Samples 149, 150) corresponding to the lower Selandian. It is marked by the LO of marker species. The disappearance of this species marks the top of the same-named DP3a subzone in the North Sea (Mudge and Bujak, 1996), which correlates with the base of the NP5 zone.

Upsection (interval of Samples of 151–166), the local Cladopyxidium saeptum zone is recognized. It is characterized by poor and low-diverse dinocyst assemblage. This assemblage is mostly composed by the species of the large stratigraphic range: common *Spini-ferites* spp., *Achomosphaera ramulifera*, *A. alcicornu*, *Impagidinium* spp., *Membranosphaera maastrichtica*, and *Batiacasphaera* spp. and rare to few *Areoligera senonensis*, *A. coronata*, *Phthanoperidinium crenulatum*, *Cladopyxidium saeptum*, *Conneximura fimbriata*, *Cerodinium speciosum*, and *Cordosphaeridium inodes*. Such a taxonomic composition of the dinocyst assemblage more likely suggests deposition in the outer shelf at a considerable distance from the coastline (Sluijs et al., 2005). The occurrence of *Cladopyxidium saeptum* and *Conneximura fimbriata* allows the correlation of the Cladopyxidium saeptum zone with the Isabelidinium? viborgense subzone DP3b of the North Sea (Mudge and Bujak, 1996).

The local Alisocysta margarita zone is defined by the FO of marker species; it is distinguished in the lower part of the undivided NP6–NP7 zones (Samples 167, 168). Its top is not recognized. In general, the composition of the dinocyst assemblage is similar to that of the underlying zone: it is characterized by the appearance of the marker species and the disappearance of *Conneximura fimbriata* and *Cladopyxidium saeptum*.

In the lower Thanetian interval of the section (from the upper part of NP6–NP7 to the base of NP9), dinocysts are not found. The Apectodinium hyperacanthum zone (Powell, 1992) is documented in the upper Thanetian sediments by occurrence of dinocysts of the genus *Apectodinium* (*A. homomorphum*, *A. quinquelatum*). The appearance of *Apectodinium* corresponds to the base of the D4c zone (Luterbacher et al., 2004), the Viborg 5 zone of the Danish Basin (Heil-

Plate II. Light microscope images of nannofossils of the Ostrich Farm section. (1) *Toweius* sp., sample 142, PL; (2) *Toweius selandianus* Perch-Nielsen, sample 148-9, PL; (3) *Toweius pertusus* (Sulivan) Romein, sample 148-5, PL; (4) *T. pertusus*, sample 126-3, PL; (5) *Toweius occultatus* (Locker) Perch-Nielsen, sample 119, PL; (6) *Toweius callosus* Perch-Nielsen, sample 8-4, PL; (7) *T. callosus*, sample 126, PL; (8) *Toweius eminens* Bramlette et Sullivan, sample 111, PL; (9) *Toweius tovae* Perch-Nielsen, sample 152, PL; (10) the same sample, OL; (11) *Toweius rotundus* Perch-Nielsen, sample 8-1, PL; (12) *Girgisia gammation* (Bramlette et Sullivan) Varol, sample 131, PL; (13) *Toweius crassus* (Bramlette et Sullivan) Perch-Nielsen, sample 132, PL; (14) the same specimen, LO; (15) *Toweius magnicrassus* (Bukry) Romein, sample 135, PL; (16) *Helicosphaera?* sp., proximal view, sample 119, PL; (17) *Helicosphaera?* sp., distal view, sample 119, PL; (18) *Helicosphaera?* sp., distal view, sample 114, PL; (19) *Ellipsolithus macellus* (Bramlette et Sullivan) Sullivan, sample 8-1, PL; (20) *Ellipsolithus distichus* (Bramlette et Sullivan) Sullivan, sample 155A, PL; (21) *Pontosphaera plana* (Bramlette et Sullivan) Haq, sample 126-3, PL; (22) *Transversopontis pulcher* (Deflandre in Deflandre et Fert, 1954) Hay, Mohler et Wade, sample 129, PL; (23) *Pontosphaera?* sp., sample 142, PL; (24) *Fasciculithus tympaniformis* Hay et Mohler, sample 148-5, PL; (25) *Fasciculithus involutus* Bramlette et Sullivan, sample 149, PL; (26) *Lithoptychius janii* (Perch-Nielsen) Aubry, sample 148-6, PL; (27) *Fasciculithus clinatus* Bukry, sample 163, PL; (28) *Lithoptychius billii* (Perch-Nielsen) Aubry, sample 151, PL; (29) *Lithoptychius ulii* (Perch-Nielsen) Aubry, sample 149, PL; (30) *Lithoptychius ulii* (Perch-Nielsen) Aubry, sample 150, distal view, PL.

Plate III

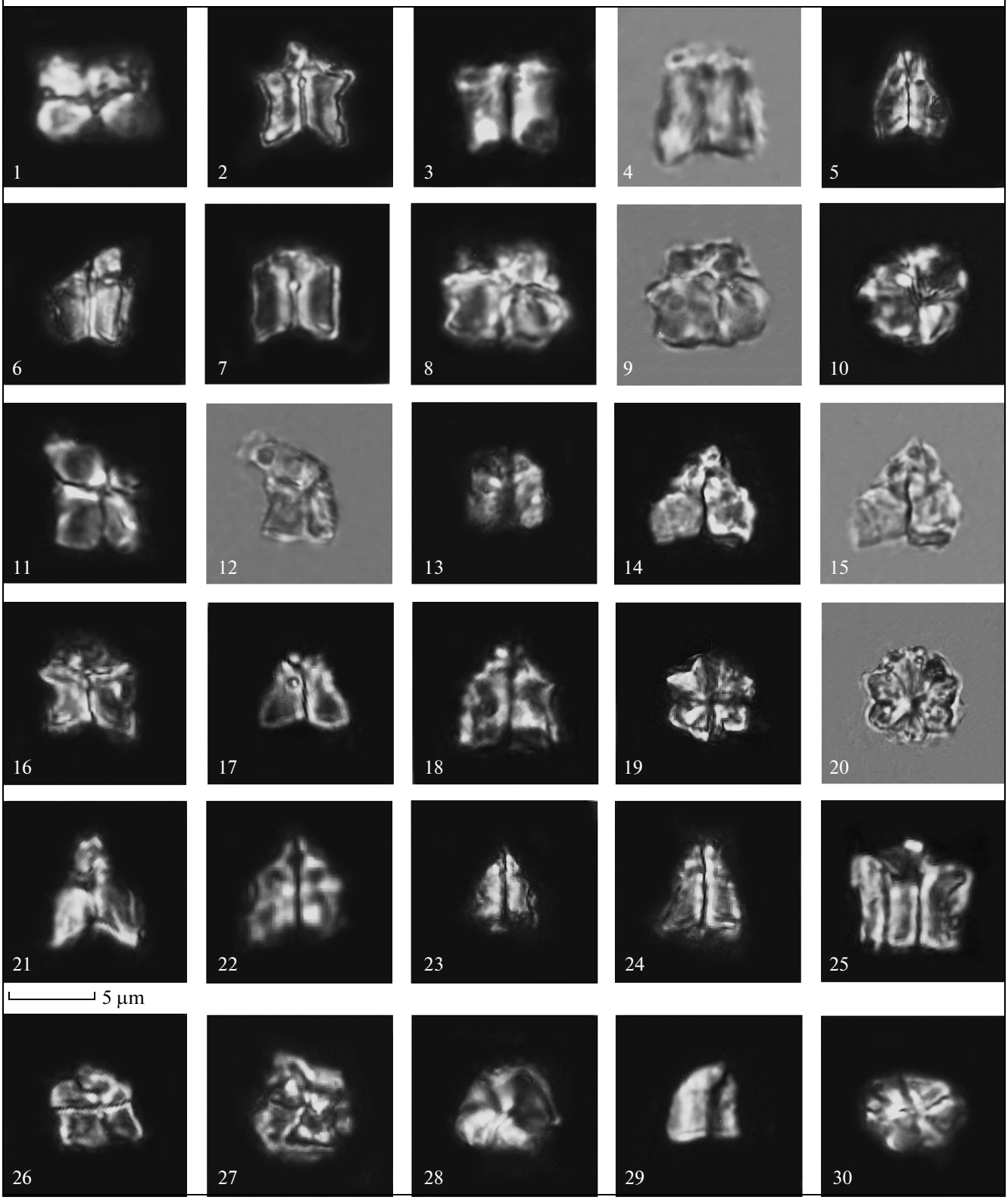
1
2
3
4
5
6
7
8
9
10
11
12
13
14
15
16
17
18
19
20
21
22
23
24
25
5 μm
26
27
28
29
30

mann-Clausen, 1994), and the Apectodinium hyperacanthum zone (Powell, 1992) and correlates to the base of the NP9 zone.

The Apectodinium augustum zone (Powell, 1992) is recognized in the lower part of the NP10 zone. It is defined in the lower part of NP10 zone by the range of marker species and *Apectodinium* acme. This Apectodinium augustum zone corresponds to the D5a zone (Luterbacher et al., 2004), the Viborg 5 zone of the Danish Basin (Heilmann-Clausen, 1994), the DP6b subzone of the North Sea Basin (Mudge and Bujak, 1996). The A. augustum biozone and the acme of *Apectodinium* in different regions of the world correspond to the negative carbon isotope excursion (CIE), which characterizes the PETM and defines the Paleocene–Eocene boundary (Crouch et al., 2001, 2003; Luterbacher et al., 2004; Aubry et al., 2007).

The lower Eocene part of the Ostrich Farm section (NP10 (upper part)–NP12) comprises two short stratigraphic hiatuses. Firstly, dinocyst study (Table 5) attest that so-called initial Eocene interval (Deflandrea oebisfeldensis dinocyst zone) is missed in the sedimentary record and the Eocene part of the section (Ypresian s.s.) begins with the FO of *Wetzeliella astra* and *W. lobisca*. Upsection, the Ypresian part of the section (NP11) is characterized by the successive occurrence of the stratigraphically important species *Biconidinium longissimum*, *Deflandrea phosphoritica* (prior to the FO of *Discoaster barbadiensis*), *Dracodinium simile*, *Rhombodinium translucidum*, *Wetzeliella uncinata* (between the FO of *D. barbadiensis* and FOs of *Coccolithus crassus* and *Discoasteroides kuepperi*), *Diphyes ficusoides*, *Dracodinium varielongitudum*, *Wetzeliella unicaudalis*, *Wilsonidium tabulatum* (approximately coinciding with the level of the FOs of *C. crassus*, *D. kuepperi*), *Dracodinium politum* (NP11, above the first occurrence of *Chiphragmalithus armatus*), and *Cerebrocysta bartonensis* (NP12, coinciding with the FO of *Discoaster lodoensis*) (Fig. 4). Accordingly, the second short hiatus corresponds to the level of the FO of *Wetzeliella meckelfeldensis* (NP11 zone).

Small Foraminifers

The planktonic foraminifer stratigraphy of the section was made using the updated Crimea–Caucasus Stratigraphic Scale (*Prakticheskoe...*, 2005). The taxonomic composition of foraminiferal assemblages and distribution of species is shown in Table 6. Occurrence of common *Parasubbotina pseudobulloides*, *Globanomalina imitata*, *Subbotina trivialis*, *Globanomalina ehrenbergii* and *G. compressa* in the lower part of section (Samples 140–149, upper Danian) indicates Praemurica inconstans zone. In its upper part, *Praemurica inconstans* is found: at the lower part, few *Globoconusa daubjergensis*, probably inherited from the underlying zone, are observed. Upward, the foraminifera assemblage entirely changes: almost all species of the precedent assemblage disappear and *Morozovella angulata*, *Subbotina triangularis*, and *Igorina albeari* appear. Above this level, (samples 151, 152), *Globanomalina pseudomenardii*, *G. chapmani*, numerous *Igorina djanensis*, and then *Acarinina subsphaerica*, *A. nitida* (=*A. acarinata*), *Subbotina velascoensis*, and *Morozovella acutispira* first occur. This part of the section (interval of Samples of 150–160) is assigned to the Igorina djanensis zone. Thus, Morozovella angulata and Morozovella conicotruncata zones are missed at the Danian and Selandian transition. The lower boundary of the Acarinina subsphaerica zone (Samples 161–015) is detected by abundant occurrence of marker species. This zone contains also species from the underlying zone, except for *I. djanensis*. Higher in the section (Samples 013–08), the Acarinina nitida zone (=Acarinina acarinata zone), ranging terminal Thanetian-initial Ypresian, is recognized. The lower boundary of this zone is tentatively defined by the disappearance (slightly below) of *Globanomalina pseudomenardii* and the occurrence of *Morozovella aequa*. Foraminifers in this interval are poorly preserved. *Morozovella* cf. *cancellata*, *M.* cf. *subbotinae*, and *Acarinina* cf. *soldadoensis* appear successively within the sedimentary record ranging this zone. The Morozovella subbotinae s.l. zone can be suggested for the Samples 07–03. The Morozovella subbotinae s.str. subzone is distinguished in the Sample 07 on the basis of abundant occurrence of the marker species. The Morozovella marginodentata subzone is identified in

Plate III. Light microscope images of nannofossils of the Ostrich Farm section. (1) *Diantholithina mariposa* Rodriguez et Aubry, sample 143, PL; (2) *Fasciculithus* sp. 1, sample 150, PL; (3) *Fasciculithus* sp. 2, sample 148-6, PL; (4) the same specimen, OL; (5) *Fasciculithus* sp. 3, sample 120, PL; (6) *Fasciculithus* sp. 4, sample 152, PL; (7) *Fasciculithus* sp. 5 sensu Bernaola et al., 2009; (8) *Diantholithina* sp. 1, sample 142, PL; (9) the same specimen, OL; (10) *Diantholithina* sp. 1, distal view, sample 142, PL; (11) *Diantholithina?* sp. 2, sample 148-6, PL; (12) the same specimen, OL; (13) *Lithoptychius chowii* (Varol) Aubry, sample 148-6, PL; (14) *Diantholithina* sp. 3, sample 128-6, PL; (15) the same specimen, OL; (16) *Lithoptychius vertebratoides* (Steurbaut et Sztrakos) Aubry, sample 148-5, PL; (17) *Fasciculithus lillianae* Perch-Nielsen, sample 116, PL; (18) *Fasciculithus richardii* Perch-Nielsen, sample 116, PL; (19) *Fasciculithus sidereus* Bybell et Self-Trail, sample 120, PL; (20) the same specimen, OL; (21) *Fasciculithus schaubii* Hay et Mohler, sample 119, PL; (22) *F. schaubii*, sample 120, PL; (23) *Fasciculithus hayi* Haq, sample 120, PL; (24) *Fasciculithus thomasii* Perch-Nielsen, sample 120, PL; (25) *Fasciculithus* sp. 6, sample 170, PL; (26) *Lithoptychius varolii* (Steurbaut et Sztrakos) Aubry, sample 170, PL; (27) *Lithoptychius* sp., distal view, sample 148-5, PL; (28) the same sample, OL; (29) *Fasciculithus* sp. 7, sample 151, PL; (30) *Lanternithus duocavus* Locker, sample 143, PL.

Table 4. Distribution of palinomorphs in Paleocene deposits (Ostrich Farm section)

Dinocyst species \ Sample no.	143	144	145	147	148	149	01.	02.	03.	04.	05.	06.	07	150	151	152	153	154	155	155A	156	157	158	159	160	162	163	164	165	166	167	170	173	110	113	116	119	120	121	122	124
Impagidinium velorum–I. elegans	23			30	4	12	1	8	36	14	15	8	9	55	10	9	9	28	13	5	3		42	7	1	35	14						15	3	3				10	4	4
Spiniferites spp.	21	26		23	20	45	21	6	35	21	17	22	3	28	29	5	15	13	5	20	4	15	78	13	8	23	8	10	5	6	t	4	9	3	4	1	1		43	54	17
Spiniferites comutus	1	5		2	1		2		2	4	2		1	2		1		5				3	4			2					2		53						1		2
Membranosphaera maastrichtica	1	6		13	6	4	6		3	10	5			2											1	6						1		1						1	1
Cordosphaeridium exilimurum	1																																		1						
Cordosphaeridium gracilis	1									1					1			1		1																			3	2	
Cordosphaeridium microtriania	9			11			6		4	2																															
cf. *Pentadinium laticinctum*	2		1																																						
Phanerodinium sonciniae	2								1																						1										
Areoligera cf. *coronata*	3						6													3						1															
Cleistosphaeridium sp.	13	3		3		1			3				2	6		2	2	1		2		3	3				3		1										1	3	
Achomosphaera ramulifera	1			4		3	4			2				3	2	2		3		2		3			1	4	3			2			3	1			3	1		1	1
Achomosphaera alcicornu	1			1	1	2	2		1	1	3		1	5	1				1				1							1			5				1		5	11	9
Achomosphaera sp.	6	5			1	1			7	3		1	6	9	1			4		3			16			12	3						3	1	1				1	3	
Florentinia ferox	1	4		3			2							1		1		1		3																					
Diphyes recurvatum	5			1		3								1		1																									
Unidentified chorate species	10	8				4							2			4		2							1								15						11	9	10
Kallosphaeridium yorubaense	4	1				1																											1								
Kallosphaeridium spp.	7	15			1	3								3		1						2			1	2						1							8	9	
Cometodinium cometes	1																														3	4								
Hystrichostrogylon coninkii	1																																							
Hystrichostrogylon cf. *borissii*	2																																							
Hafniasphaera septata	2	2						1												1								1									1	2	1	
Oligosphaeridium complex	3	2													1											2						3								
Fibradinium anettorpense	12	25	1											1																										
Microdinium cf. *dentatum*	2	1																								1														
Cladopyxidium saeptum	2	9		1		6			5	2	1	1	4	3	2	8	2			1		4		1	2	6														
Operculodinium centrocarpum	7	8			12	9	16	3					1	3	1					11		1	9							2			13						4	6	
Operculodinium sp.	3	1								5	1			3		1																							1	3	
Alterbidinium sp.	2																																	1					1		
Hystrichosphaeridium tubiferam	3			10	1	8	2			4	2	1				4		3		1		1	6		1					1			1		1					
Hystrichosphaeridium sp.	2																	2		1					1															
Alisocysta reticulata	1	14	2							1																															

Table 4. (Contd.)

Dinocyst species \ Sample no.	143	144	145	147	148	149	01.	02.	03.	04.	05.	06.	07	150	151	152	153	154	155	155A	156	157	158	159	160	162	163	164	165	166	167	170	173	110	113	116	119	120	121	122	124
Alisocysta sp. 1 Heilmann-Clausen	1	3																																							
Trithyrodinium evittii	2																																								
Polysphaeridium sp.	1																																								
Danea mutabilis	1												1																												
aff. *Achilleodinium* sp.		3																																							
Cordosphaeridium sp.		2							4			1			1											4													1		
Cordosphaeridium funiculatum		10																				1				2														
Cordopshaeridium multispinosum		6																																							
Achomosphaera crassipellis		4																																							
Spinidinium densispinatum		8				1			1	2			1			2																									
Spinidinium ornatum		3																																							
Spinidinium essoi		1																																							
Spinidinium sp.		1				2						1																											4		
Cerebrocysta sp.		5					1	2	10	6	5	3	3	2			6				3	5	22		6	6	1								1				2		
Xenikodimum lubricum		2	1																																						
Xenikodinium rugulatum		2		1					1																																
Impagidinium pentahedrias		3												8						2		9				1	3	4	1						2					
Lanternosphaeridium radiatum		1																																							
Cerodinium diebelii		3	1					1											1																					
Cerodinium speciosum		1		2														5	1				8				8	4	5	2									
Alisocysta sp.		5																																							
Senegalinium cf. *psilatum*		6																																							
Palaeoperidinium sp.			1																																						
Fibrocysta vectense			1		5	2					1		1										2															3		
Cerodinium sp.				2					1																							2								
Adnatosphaeridium sp.				2																																			1	
Cordosphaeridium inodes				3						1													1																
Hystrichosphaeridium sp. 1				2																																					
Hafniasphaera cryptovesiculata				9	12										1																									
Spinidinium cf. *densispinatum*				5										5	2		3			4		4	15		4	30	20	3	1	5					10					17
Hafniasphaera graciosa				11	5				1																							2						9		
Batiacasphaera sphaerica				1	1						1			4			1			1		5	4	3		3	9	1							2					4

Table 4. (Contd.)

Dinocyst species \ Sample no.	143	144	145	147	148	149	01.	02.	03.	04.	05.	06.	07	150	151	152	153	154	155	155A	156	157	158	159	160	162	163	164	165	166	167	170	173	110	113	116	119	120	121	122	124
Cordosphaeridium ucinispinosum				1																	2																			
Phthanoperidinium crenulatum				1			1		7	3											1	7	15	4	1	21	3		5				1	1					28	17	
Palaeocystodinium lidiae				9						2						3	1																							
Impletosphaeridium sp.					3																					1														
Nematosphaeropsis sp.					1																																			
Batiacasphaera cf. *baculata*						1			23	15	6	3	4	23	2	3	1	7		6	2	10	30	3	9	28	24	6	11	9	3	2	23	1	7	2			3		
Melitasphaeridium sp. 1						1																																		
Areoligera coronata						2																	1																	
Areoligera sp.						1														7						1			1						3					
Fibrocysta sp.						7	2										2			1						3														2
Glaphyrocysta cf. *pastielsii*						2			1																															
Melitasphaeridium simpulum							1																																	
Palaeocystodinium australinum							1			1					1								2																	
Cribroperidinium muderogense							2										1																							
Elytrocysta druggii							1																																	
Rottnestia borussica							1																																	
Diphyes pseudocolligerum									1			1		3								1		2								5								
Areoligera senonensis									1											1			2						2											
Apteodinium sp.									1													1																	
Pterodinium cf. *premnos*									9	3	1														1								4							
Hystrichokolpoma sp.										1																												1		
Elytrocysta brevis											1									6		4	4						4											13
Cleistosphaeridium diversispinosum											8																													
Glaphyrocysta sp.												2												1																
Thalassiphora delicata												1																				1								
Impagidinium spp.													1															10	4			2	2					2	1	
Cordopshaeridium fibrospinosum														1																									
Senegalinium cf. *dubium*															1																								
Hystrichosphaeridium palmatum																2																							
Achomosphaera sp. A																	1						19							7										
Cerodinium striatum																		1								1			2										
Conneximura fimbriata																		1		1												1							
Melitasphaeridium pseudorecurvatum																		1											1						1			2	
Elytrocysta sp.																				1																			
Cerebrocysta sp. 2																							30											1					
Senegalinium sp.																								1									3							

Table 4. (Contd.)

Dinocyst species \ Sample no.	143	144	145	147	148	149	01.	02.	03.	04.	05.	06.	07	150	151	152	153	154	155	155A	156	157	158	159	160	162	163	164	165	166	167	170	173	110	113	116	119	120	121	122	124
Cribroperidinium sp.																									2	1										1					
Spinidinium cf. *clavum*																										1		2												
Spinidinium cf. *sattigula*																										1														
Areoligera cf. *senonensis*																										8														2
Palaeotetradinium minusculum																										1	1													
Xenikodinium reticulatum																											1	2												
Impagidinium dispertitum																													1	1			5						5		
Glaphyrocysta ordinata																														1											
Alisocysta margarita																															7		4								
Alisocysta sp. 2 Heilmann-Clausen																																	2			1					
Wilsonidium sp.																																			1						
aff. *Cribroperodinium* sp.																																							2	8	
aff. *Enneadocysta* sp.																																						13	2	1
Glaphyrocysta exuberans																																							1	
Senegalinium obscurum																																							3	
Apectodinium quinquilatum																																						4	1	
Apectodinium sp.																																						5	2	
Gen sp. C (ex gr. *Danea*)																																						1	3	12
Caligodinium aceras																																						2	4	
Gen sp. A (ex gr. *Senoniasphaera*)																																							1	
Gen sp. A (ex gr. *Membranophoridium*)																																						3		22
Wilsonidium pechoricum																																								2
Adnatosphaeridium vittatum																																								4
Apectodinium augustum																																								1
Wetzeliella meckelfeldensis																																								1
Wetzeliella cf. *lunaris*																																								1
Dracodinium sp.																																								3
Fromea laevigata																						1		2		1		1												
Paralecaniella indentata																						1																		
Microforarniniferal linings	25	21		31	12					1		1			5	1				9		21	4	25	28	1				1			5							
Acritarchs	3	3			1	1									4	2		1					1	1	1															
Palambages sp.	3								1																															
Pterospermella sp.						4																		1															5	
Leiosphaeridia, Tasmanites												1				3										1													1		
Spores et pollen—**in situ**	11	10		16	23	11	3	1	18	9	8	4		9	10	5	11	8	3		12	40	38	49	19	22	15	15	20	49	29	5	7	9	20	3		30	62	6
Spores et pollen—**rework**	2			15	7	11	7	3	27	19	8	8		20		11		20		13		19	38	8	47	56	21	8	2	2	2		6		3			20	26	8
Dinocysts rework	4	2	1	7	1	8	4		1	2	3	2		2		2		2						2		12	3		1									4	3	1

Table 5. Distribution of palynomorphs in Lower Eocene deposits (the Ostrich Farm section)

Numbers of samples / Dinocyst species	*Apectodinium* cf. *augustum*	*Apectodinium hyperacanthum*	*Apectodinium quinquelatum*	*Cleistosphaeridium polypetellum*	*Damassadinium* cf. *impages*	*Deflandrea oebisfeldensis*	aff. *Heslertonia heslertonensis*	*Kallosphaeridium orchiense*	*Wetzeliella astra*	*Biconidinium longissimum*	*Deflandrea phosphoritica*	*Emmetrocysta* Edwards 83	*Hystrichostrogylon holohymenium*	*Wetzeliella lobisca*	*Systematophora* sp. 1 CHC-LC 89	*Wetzeliella astra-lobisca*-group	*Apectodinium homomorphum*	*Cleistosphaeridium diversispinosum*	*Apectodinium augustum-hyperacanthum*	*Dracodinium simile*	*Membranophoridium perforatum*	*Wetzeliella lunaris*	*Caligodinium amiculum*	*Deflandrea eocenica*	*Glaphyrocysta* aff. *semitecta*	*Wetzeliella meckelfeldensis*	*Arachnodinium* sp.	*Rhombodinium translucidum*	*Wetzeliella uncinata*	*Adnatosphaeridium vittatum*	*Diphyes ficusoides*	*Dracodinium* cf. *varielongitudum*	*Wilsonidium* cf. *tabulatum*	*Dr. simile-varielongitudum*	*Dracodinium varielongitudum*	*Wetzeliella unicaudatis*	*Wilsonidium* aff. *echinosuturatum*	*Wilsonidium tabulatum*	*Dracodinium rotundum*	*Dracodinium waipawaense*	*Dracodinium* aff. *waipawaense*	*Charlesdowniea* sp.	*Dracodinium politum*	*Dr. rotundum-waipawaense-politum*	*Adnatosphaeridium multispinosum*	*Adnatosphaeridium robustum*	*Cerebrocysta bartonensis*
2				2	0	1		1				3															0							2												0
133				4	0		1			0																																					
3				0	2					1		2										6																								
132					1					1	2											23																								
4				1	5		1			2	0	1										7																								
131					1					1												43																								
5				9	1		1			1	2	2									2	5					3																		
130				0	1		1							0			1				4	10					0																		
8/13			1	1	1	1						3						3			8											0												
8/12			0		4	0				2											4	3	1									1	0	0	18								
3/11			1	5	2							2			9	6					1																							
127				1	0		2					3		0		5					0		1																					
8/9			4	40								13					2							2	2	1																	
7				10							1	6					2	1	1	1			1																				
8/8			9				I					1	1			8																											
8/7			1		0		2					1		3	0																												
8/6			0	4			4		6			3																														
7a	9			10	4		8					18		1	1			1																									
8/5				5	1		0					7	0			22	1																									
8/4	1			4	1	1		1			2	2			1	13																										
8/2			17		1	0			3	1	4	1	1	6																												
8/1	2	11	1	0	0	0	1	2	5																																

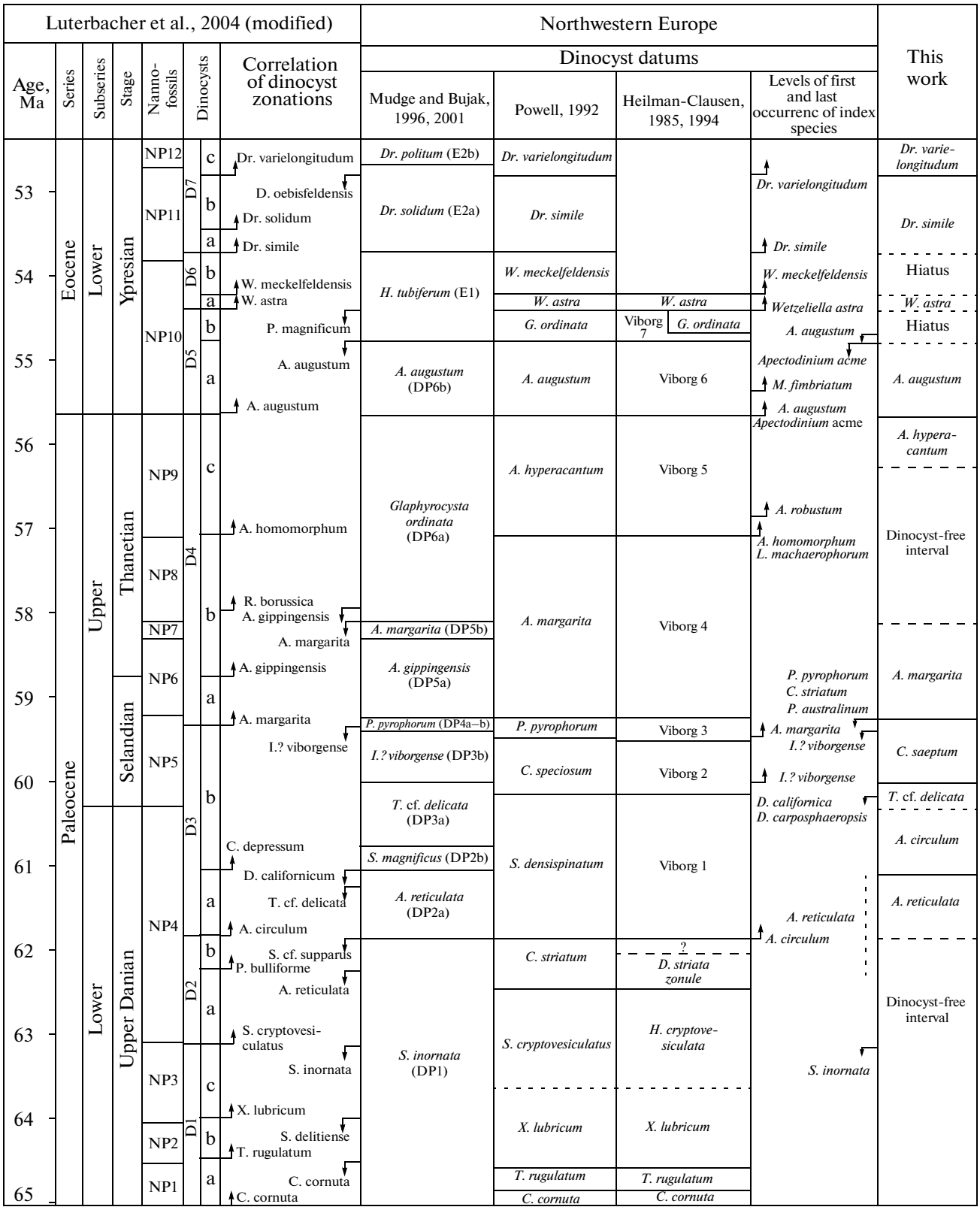

Fig. 6. Correlation of the Paleocene–Eocene dinocyst zonations. The position of the Danian–Selandian boundary was changed according to the decision of International Committee on Paleogene Stratigraphy (Schmitz et al., 2011).

Table 6. Distribution of main species of planktonic foraminifera in the Paleocene–lower Eocene deposits (Ostrich Farm section)

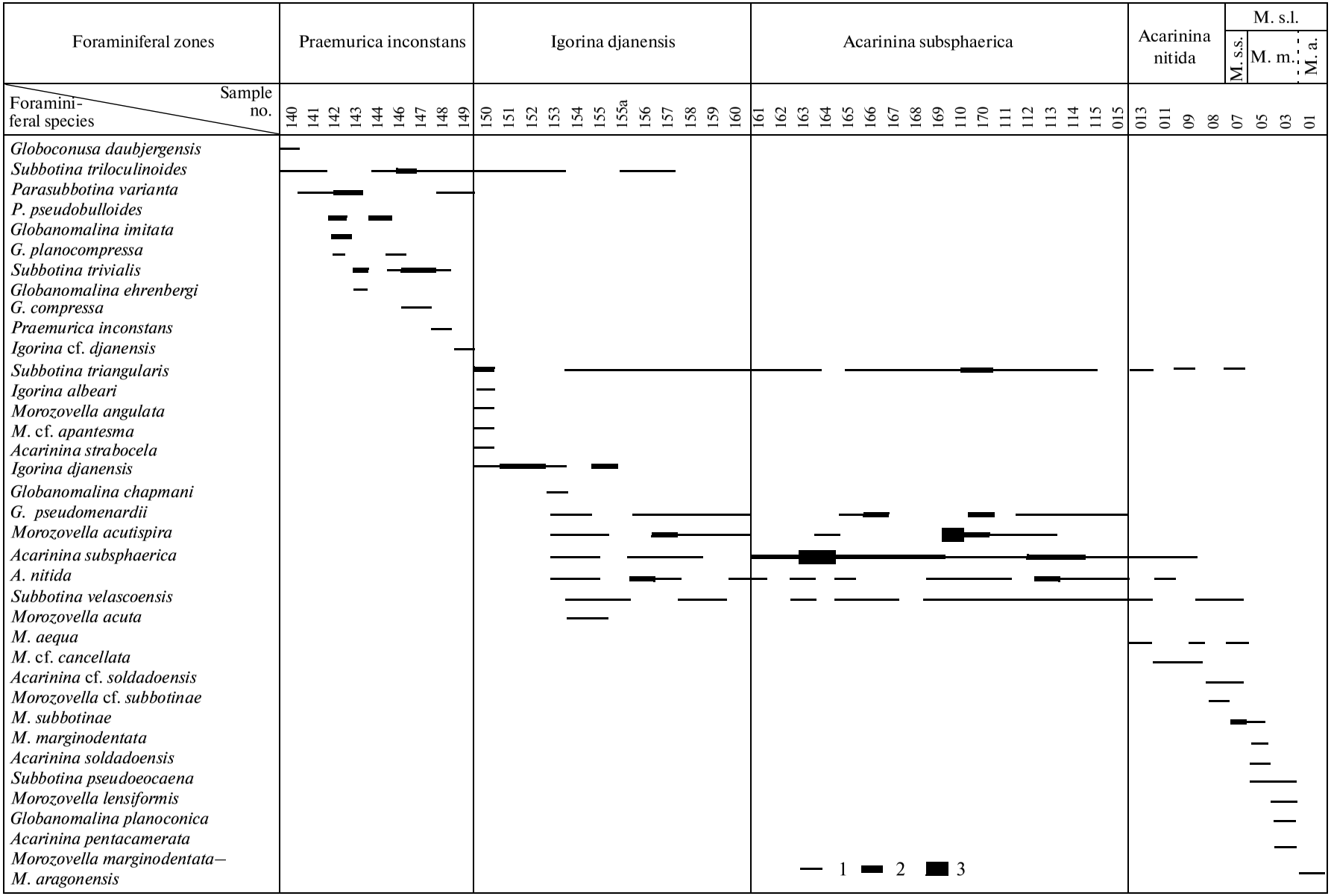

Number of representatives: (1) rare (1–5 representatives in a weight); (2) many (6–10 representatives in a weight); (3) numerous (11–15 representatives in a weight).
Abbreviations: *M.* s.l.—*Morozovella subbotinae* s.l.; *M.* s.s.—*Morozovella subbotinae* s.str.; *M. m.*—*Morozovella marginodentata*; M. a.—*Morozovella angulata*.

the interval of the Samples 06–03 on the basis of the appearance of *Morozovella lensiformis*, *Subbotina pseudoeocaena*, *Globanomalina planoconica*, and *Acarinina pentacamerata* marker species. In the Sample 01, the transitional forms of *Morozovella marginodentata–Morozovella aragonensis* (with five chambers in the last whorl and strongly exserted umbilical side) were identified. This part of the section can be likely attributed to the Morozovella aragonensis zone.

Benthic foraminifers are not common and represented mostly by poorly preserved shells.

In the lowermost part of the section (Samples 140, 141), benthic foraminifers were not found; in Sample 142, *Rhabdammina* sp., *Ammodiscus* sp., *Reptamina charoides*, *Heterostomella gigantica*, *Spiroplectammina* sp., *Lenticulina* sp., *Nuttallides truempyi*, *Gavelinella beccariiformis*, and *Brotzenella praeacuta* were identified. Upsection, *Allomorphina* sp. (Sample 146), *Cibicidoides alleni* (Sample 150), *Clavulina parisiensis, Haplophragmoides subsphaeroides, Neoflabellina semireticulata, Pullenia americana, Anomalinoides danicus* (Sample 154), *Spiroplectammina kortishensis limbosa*, *Lituotuba lituiformis*, *Stilostomella midwayensis*, *Pullenia quinqueloba*, and *Cibicidoides succedens* (Sample 110) appear. In Sample 08, most of the foraminifer shells (mainly rotaliides) are crushed and ferruginated. *Gavelinella beccariiformis*, the species, which became extinct near the Paleocene–Eocene boundary, disappear at this level. The overlying deposits (Samples 07–01) contain the foraminiferal assemblage represented by *Rhabdammina* sp., *Ammodiscus* sp., *Subreophax splendida*, *Pseudogaudryina* sp., *Nuttallides truempyi*, *Anomalinoides* sp., and *Cibicidoides* sp. In general, the low-diversity benthic foraminiferal community is of the Midway (offshore) type fauna, although it contains some species of the Velasco bathyal fauna (*Nuttallides truempyi*, *Gavelinella beccariiformis*) (Berggren and Aubert, 1975). In the overlying deposits, foraminifers were not found.

Large Foraminifera

Large benthic foraminifera were found during microscopic observations of the thin sections of lower Ypresian and Lutetian deposits. The most complete foraminiferal community was identified in washed Sample 8/5 (calcareous clays), containing planktonic foraminifers of the early Ypresian Morozovella subbotinae zone. Large foraminifera are represented by very small (0.7–2 mm), sometimes rounded shells with incomplete number of whorls (nummulitides) or equatorial cyclical chambers (orthophragminides). The chambers are often filled with glauconite; drilling traces in shells are rare. All foraminiferal species, except for rare *Nemkovella* species, belong to the megaspherical generation. Among nummulites, the species of *Nummulites globulus* group dominate: *N. soerenbergensis* Schaub, 1951 and *N.* cf. *increscens* Schaub, 1951, 1846; *N. praelucasi* Douville, 1924 and *N.* cf. *pernotus* Schaub, 1951 are less common. Rare operculines are represented by *Operculina karreri* Penecke, 1885. Orthophragminids are more diverse and represented by *Orbitoclypeus schopeni crimensis* Less, 1987, *O. douvillei yesilyurtensis* Özcan, 2002, *O. varians portnayae* Less, 1987, *Nemkovella evae* Less, 1987, *N. strophiolata indet* ssp., *Discocyclina augustae sourbetensis* Less, 1987, and *D. archiaci* cf. *archiaci* (Schlumberger, 1903).

Nummulites of this association are typical for the upper Ilerdian and lower Cuisian (this interval corresponds to the nannofossil NP12 zone). Most of the orthophragminides are represented by Ypresian transitional subspecies. Some features (a small diameter of the embryonic apparatus in *Orbitoclypeus schopeni crimensis*, relatively common *O. varians portnaya*, and occurrence of *Discocyclina archiaci* cf. *archiaci*) indicate early Cuisian age of this community, but occurrence of subspecies *O. douvillei yesilyurtensis* in this assemblage contradicts this assumption. This subspecies was established in the middle Cuisian deposits of Turkey and the North Caucasus (the lower boundary of the NP13 nannofossil zone) only. Besides nummulitides and orthophragminides, occurrence of rare acervulinids of the genus *Sphaerogypsina* characterizes this assemblage of large foraminifera.

The morphotype of large foraminifera (small dimensions of the shell and embryo) evidences long-lived unfavorable conditions of their habitat. Rare species of large foraminifera belonging to genera *Orbitoclypeus* and *Discocyclina* were identified in other samples from the Ypresian interval, and at the base of Lutetian diatomite-spongolite sequence, they are represented by the genera *Nummulites*, *Orbitoclypeus*, *Nemkovella*, and *Discocyclina* (Plate I, figs. 21–24).

DISCUSSION

The detailed study of the Paleogene sediments of the Urma Plateau, containing high-diversity assemblages of three groups of microplankton, enabled the definition of exact stratigraphic range of the Paleogene deposits, subdivision of this succession on the basis of detailed zonations, definition of the range of hiatuses and correlation of the nannofossil, dinocyst and foraminifer datums (Fig. 7).

Abundant and diverse dinocyst assemblage found in the lower part of Ostrich Farm section demonstrate high evolutionary rate, while nannofossil and foraminiferal assemblages are rather poor quantitatively, although their taxonomical diversity is reliable to

Plate IV

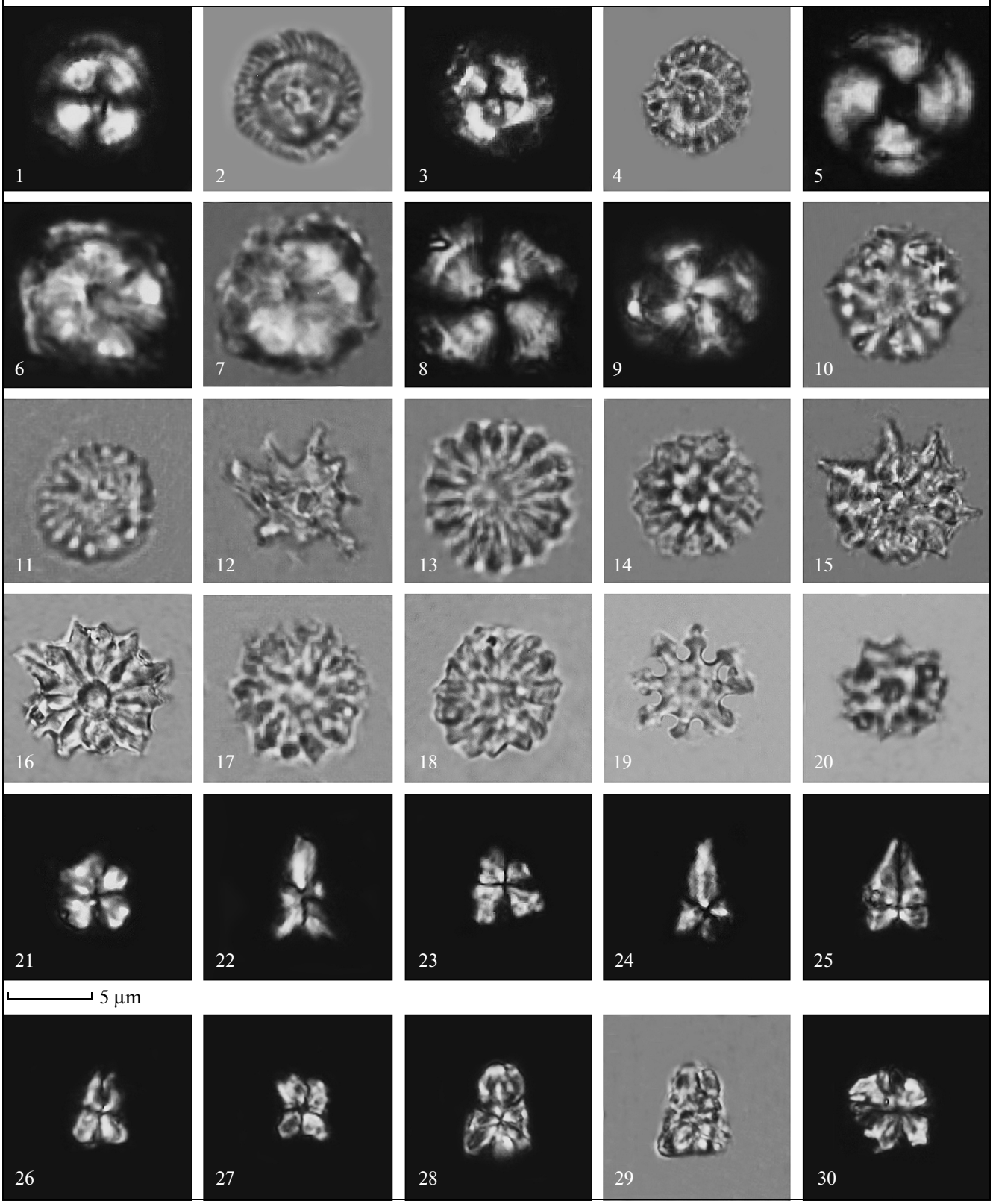
1
2
3
4
5
6
7
8
9
10
11
12
13
14
15
16
17
18
19
20
21
22
23
24
25
5 μm
26
27
28
29
30

define zonal subdivisions. Vice versa, nannofossil and foraminifer diversity greatly increases within the marl unit, while dinocysts become less abundant.

In the studied part of the Danian deposits, the marker species (*Ellipsolithus macellus*) of the NP4 zone of the nannofossil standard scale (Martini, 1971) was not found, that is typical for the entire Crimea-Caucasus Region (Muzylev, 1981). For this reason, N.G. Muzylev assigned the upper part of Danian deposits to the Coccolithus robustus zone, which roughly ranges the NP4 zone. At the same time, our study showed that this interval can be subdivided into three subzones of a more detailed Danian zonation developed by O. Varol (NTp7A–NTp8A) for the North Sea Basin. Noteworthy, this scale was successfully applied for detailed subdivision of Tethian sections (Steurbaut and Sztrakos, 2008; Bernaola et al., 2009; Sprong et al., 2009; Youssef Ali, 2009). The standard Martini zonation can be reliably used for subdivision of the upper Paleocene–lower Eocene sequences (Martini, 1971). The Middle Eocene part of the section can be confidently dated using Okada and Bukry standard zonation (1980), more reliable and detailed for this interval.

As it was noted, foraminiferal zonation elaborated for the Crimea–Caucasus area and recently updated by E.M. Bugrova (*Prakticheskoe...*, 2005) was applied for sections studied. The use of regional zonation is caused by the absence or sporadic occurrence of warm-water foraminiferal key species served for zonal definition in zonations elaborated in tropical area (Berggren and Pearson, 2005; previous works by Bolli, Blow, and others (see references incited)). The foraminiferal zones of the Crimea–Caucasus scale, which is useful also in the Central Asia, were originally compiled on the basis of the composition of foraminiferal assemblage, where zonal boundary could be defined by common occurrence of marker species, although its rare occurrence might took place in the underlying zone. Despite evident inconvenience in such zonal boundaries, this concept seems to be optimal for polyfacial deposits of the epeiric basin, partly isolated from the Tethian realm.

The proposed zonal subdivisions of the "detailed" scale of the Crimean–Caucasian region, developed using datum planes (Beniamovskii, 2001; Akhmetiev and Beniamovskii, 2006), cannot be identified in the studied section.

Basically, the succession of the FOs of nannofossil species revealed in the upper Danian sediments is similar to the evolutionary succession documented in different basins of Tethyan realm. However, the first radiation of fasciculiths, clearly identified in many parts of the Tethys prior to the base of NTp7b subzone (Steurbaut and Sztrakos, 2008; Bernaola et al., 2009; Sprong et al., 2009), is not documented in the section studied, although extremely rare specimens of fasciculiths similar to *Lithoptychius chowii* (Plate III, fig. 13) are found at the level of the FO of *Chiasmolithus edentulus* (~23 m below the Danian–Selandian boundary). Probably, the event of 1st radiation of fasciculiths falls to the unsampled part of the section, disturbed by submarine slumping. The same processes could be responsible for the high position of the lower boundary of the NTp7B subzone and thus of reduction of its true stratigraphic range in the section. Other early fasciculiths, recently assigned to the genera of *Diantholithina* and *Lithoptychius* (Aubry et al., 2011), were identified in the deposits of the NTp8A subzone (Plate III). This level is significantly higher than the interval of distribution of both these genera in Egypt, where it is mainly restricted to the NTp7B subzone (Aubry et al., 2012).

The occurrence of common *Sphenolithus primus*, which marks the base of the NTp8A subzone, coincides with the very early FO of bomoliths similar to *Bomolithus elegans*. Bomoliths are thought to be transitional morphotype between fasciculiths and helioliths, which usually appear in the Selandian NP5 zone (Perch-Nielsen, 1985), although the occurrence of these species was found in the uppermost Danian deposits in SW France (Steurbaut and Sztrakos, 2008). The occurrence of bomoliths at a much lower

Plate IV. Light microscope images of nannofossils of the Ostrich Farm section. (1) *Bomolithus elegans* Roth, sample 144, PL; (2) the same specimen, OL; (3) *Bomolithus conicus* Perch-Nielsen, sample 149, PL; (4) the same specimen, OL; (5) *Heliolithus floris* Haq et Aubry, sample 114, PL; (6) *Heliolithus cantabriae* Perch-Nielsen, sample 151, PL; (7) the same specimen, OL; (8) *Helio-lithus kleinpellii* Sullivan, sample 165, PL; (9) *Helioithus riedelii* Bramlette et Sullivan, sample 170, PL; (10) *Discoaster mohleri* Bramlette et Percival, sample 170, OL; (11) *Discoaster mohleri* Bramlette & Percival, sample 111, OL; (12) *Discoaster anartios* Bybell et Self-Trail, sample 08, OL; (13) *Discoaster multiradiatus* Bramlette et Riedel, sample 123, OL; (14) *Discoater salisburgensis* Stradner, sample 124, OL; (15) *Discoaster limbatus* Bramlette et Sullivan, sample 125, OL; (16) *Discoaster diastypus* Bramlette et Sullivan, sample 8-4, OL; (17) *Discoaster barbadiensis* Tan Sin Hok, sample 129, OL; (18) *Discoaster elegans* Bramlette et Sullivan, sample 8-5, OL; (19) *Discoaster binodosus* Martini, sample 9A, OL; (20) *Discoasteroides kuepperi* (Stradner) Bramlette et Sullivan, sample 130, OL; (21) *Sphenolithus primus* Perch-Nielsen, sample 143, PL; (22) *Sphenoithus* sp. 1, sample 127, PL; (23) *Sphenolithus moriformis* (Bronniman et Stradner) Bramlette et Wilcoxon, sample 128, PL; (24) *Sphenolithus radians* Delfandre in Grassé, sample 129, PL; (25) *S. radians*, 1952, sample 131, PL; (26) *Sphenolithus orphanknollensis* Perch-Nielsen, sample 132, PL; (27) *Sphenolithus stellatus* Gartner, sample 27, PL; (28) *Sphenolithus* sp. 2, sample 134, PL; (29) the same specimen, OL; (30) *Sphenolithus* sp. 3, sample 131, PL.

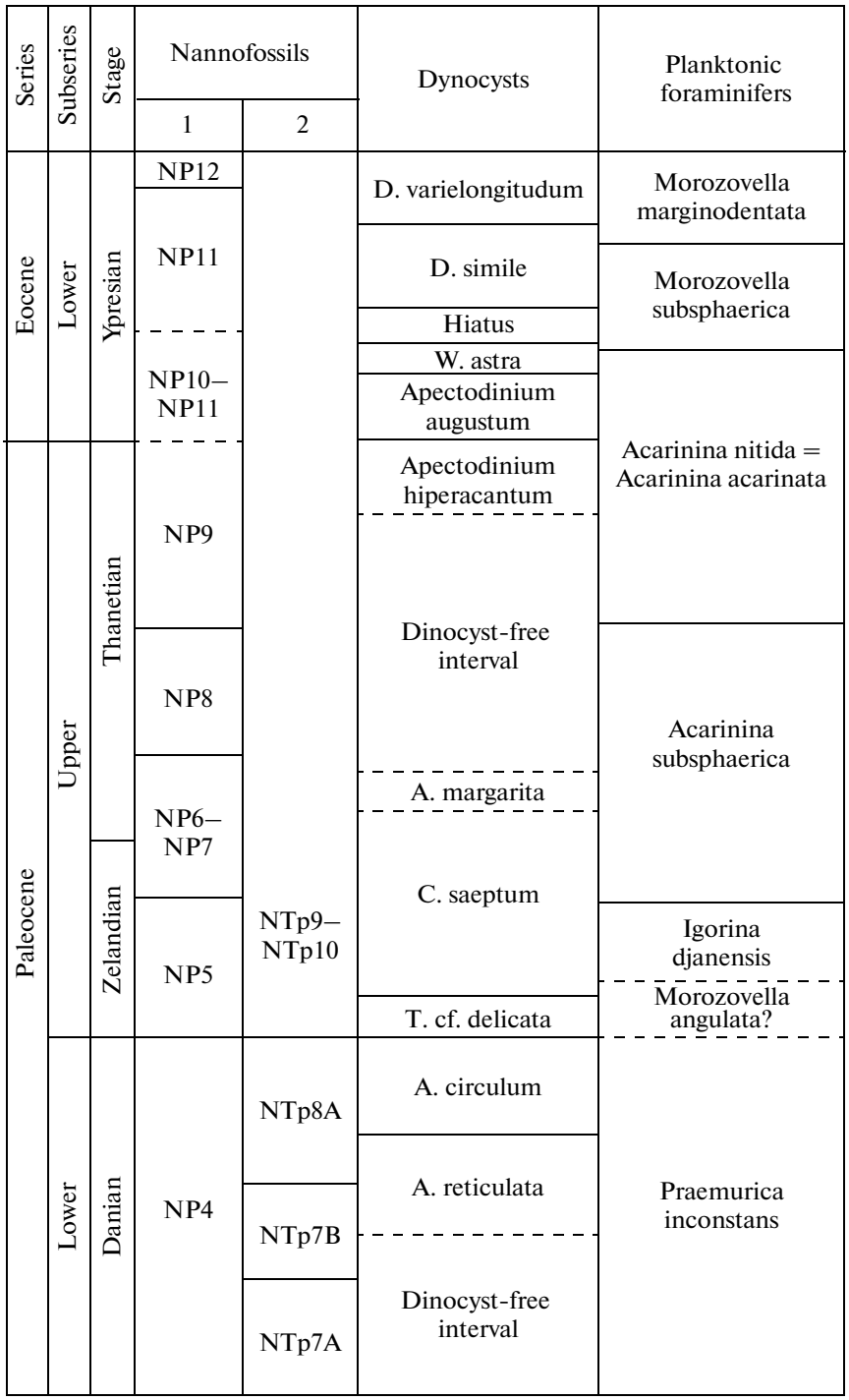

Fig. 7. Correlation of nannofossil, dinocysts, and planktonic foraminifers zonations in the Ostrich Farm section. (1) Martini zonation (Martini, 1971), (2) Varol zonation (Varol, 1989).

stratigraphic level may be the evidence of early evolutionary evolutionary separation of Momolithus lineage at a very early stage of fasciculith evolution prior to their bloom.

In some areas, e.g., in the sections of Denmark and the Basque Country, the interval of NTp7A–NTp8A subzones is characterized by mass occurrence (acme) of *Braarudosphaera bigelowii* (Clemmensen and Thomsen, 2005; Bernaola et al., 2009), culminating at the boundary of the NTp8B/NTp8C subzones. However, in the southern margin of the Tethys, this phenomenon was not observed (Sprong

et al., 2009; Youssef Ali, 2009). In the Ostrich Farm section, this interval is characterized by common and diverse pentaliths (braarudosphaerids and micrantoliths), although it is not real mass occurrence and they become declined at the level ~5.5 m below the base of marl sequence. The 2nd radiation of fasciculithes was recorded in the uppermost Danian deposits of the Boreal and Tethian realms (Varol, 1989; Steurbaut and Sztrakos, 2008; Bernaola et al., 2009; Youssef Ali, 2009). It corresponds to boundary of the NTp8B and NTp8C subzones. However, in the uppermost Danian deposits of our section, fasciculiths are not found; late Danian species (*L. ulii*, *L. janii*, *L. billii*) occur at the base of marl sequence together with marker species of the base of Selandian NP5 zone *Fasciculithus tympaniformis*. This suggests a hiatus at the Danian/Selandian boundary ranging NTp8B–NTp8C subzones in the Ostrich Farm section and earlier termination of pentalith common occurrence in the upper part of the NTp8A subzone.

The first occurrence of dinocysts in the section coincides with the boundary of the NTp7B/NTp8A subzones. The NTp8A subzone corresponds to two local dinocyst zones: Alisocysta reticulata and Alterbidinium circulum, which can be correlated to three subzones of the North Sea zonation: DP2a Alisocysta reticulata, DP2b Spiniferites magnificus, and DP3a Thalassiphora cf. delicata (Mudge and Bujak, 1996). In the Ostrich Farm section, the upper boundaries of the DP2a (the LO of *Alisocysta reticulata*) and DP3a (the LO of *Thalassiphora* cf. *delicata*) subzones were documented. However, the boundary between the DP2b and DP3a subzones was not recognized due to not-occurrence of the marker species (*Spiniferites magnificus*), which can be caused by a hiatus in sedimentation. According to (Powell, 1992), the LO of *Alisocysta reticulata*, *Xenicodinium lubricum*, and *Hafniasphaera cryptovesiculata* is recorded within the Cerodinium striatum zone, and the LO of *Thalassiphora* cf. *delicata* is noted in the upper part of this zone. The dinocyst zone Thalassiphora cf. delicata is correlated to the top of the NP4 zone (Powell, 1992). In general, these events were recognized in our material, except for the later LO of *Thalassiphora* cf. *delicata* at the base of the NP5 zone, which is in agreement with the data obtained from the North Sea (Mudge and Bujak, 1996) and Denmark (Thomsen and Heilmann-Clausen, 1984). The late Danian Alterbidinium circulum zone is restricted to the Danian, that is confirmed by Vasilyeva (2010) and our data. The FO of *Alterbidinium circulum* corresponds to the middle part of the NP4 zone (Luterbacher et al., 2004; Vasilyeva and Musatov, 2008; Vasilyeva, 2010).

The lower part of the section corresponds to the foraminiferal Praemurica inconstans zone according to the Crimea–Caucasus zonal scheme, ranging the upper part of the Danian. The marker species occurs in the upper part of this zone only at the level of the FOs of *Prinsius bisulcus* and *Toweius selandianus* and the LO of *Hafniasphaera cryptovesiculata*.

The transition between Danian limestone and marl sequence is a drastic lithological boundary. The application of Varol's detailed zonation evidenced the short stratigraphic hiatus ranging NTp8B–NTp8C subzones. However, there are no significant variations in nannofosil assemblage. In terms of foraminiferal zonation, the hiatus ranges the late Danian Morozovella angulata zone to early Selandian M. conicotruncata zone. Above the Danian–Selandian boundary, the total abundance of nannofossils increases significantly. However, the recognition of the NTp9 and NTp10 zonal boundary is hardly possible, because marker species of their upper boundaries are not found or scarce in this part of the section. The only exception is *Neochiastozygus perfectus*, whose stratigraphic range appeared to be larger than its range in the Norwegian Sea, where these zones were originally established. Its LO defines the top of the NTp10 zone; in the Ostrich Farm section, it disappeared later at the level of the NP6 zone. The successive FOs of *Toweius tovae* and *T. eminens* above the Danian/Selandian boundary at 2.8 and 12.0 m, respectively, is recorded evidently at the levels similar to those in the Zumaya section, Northern Spain (Bernaola et al., 2009). However, in SE France, *T. tovae* was referred in the upper Danian below the FO of *F. tympaniformis* (Steurbaut and Sztrakos, 2008).

The local dinocyst Cladopyxidium saeptum zone ranges the most of Selandian and lower Thanetian deposits, i.e., the NP5 and the lower part of the NP6 nannofossil zones, and the Igorina djanensis and the lowermost part of Acarinina subsphaerica planktonic foraminifer zones. The low abundance and taxonomic diversity of dinocysts do not allow reliable subdivision of this part of section in terms of dinocyst zonation. The assemblage of this zone differs substantially from coeval assemblages of other regions by the absence of marker species *Isabelidinium? viborgense*, *Palaeoperidinium pyrophorum*, *Areoligera gippingensis*, and *Palaeocystodinium bulliforme* (Heilmann-Clausen, 1985, 1994; Powell, 1992; Mudge and Bujak, 1996; Luterbacher et al., 2004), that could be caused by paleogeographic peculiarity of the basin. The occurrence of the secondary markers (*Cladopyxidium saeptum*, *Conneximura fimbriata*) identified in the DP3b subzone (Isabelidinium? viborgense) (Mudge and Bujak, 1996) enable partial correlation of the local Cladopyxidium saeptum zone to the Cladopyxidium saeptum subzone of the North Sea.

Plate V

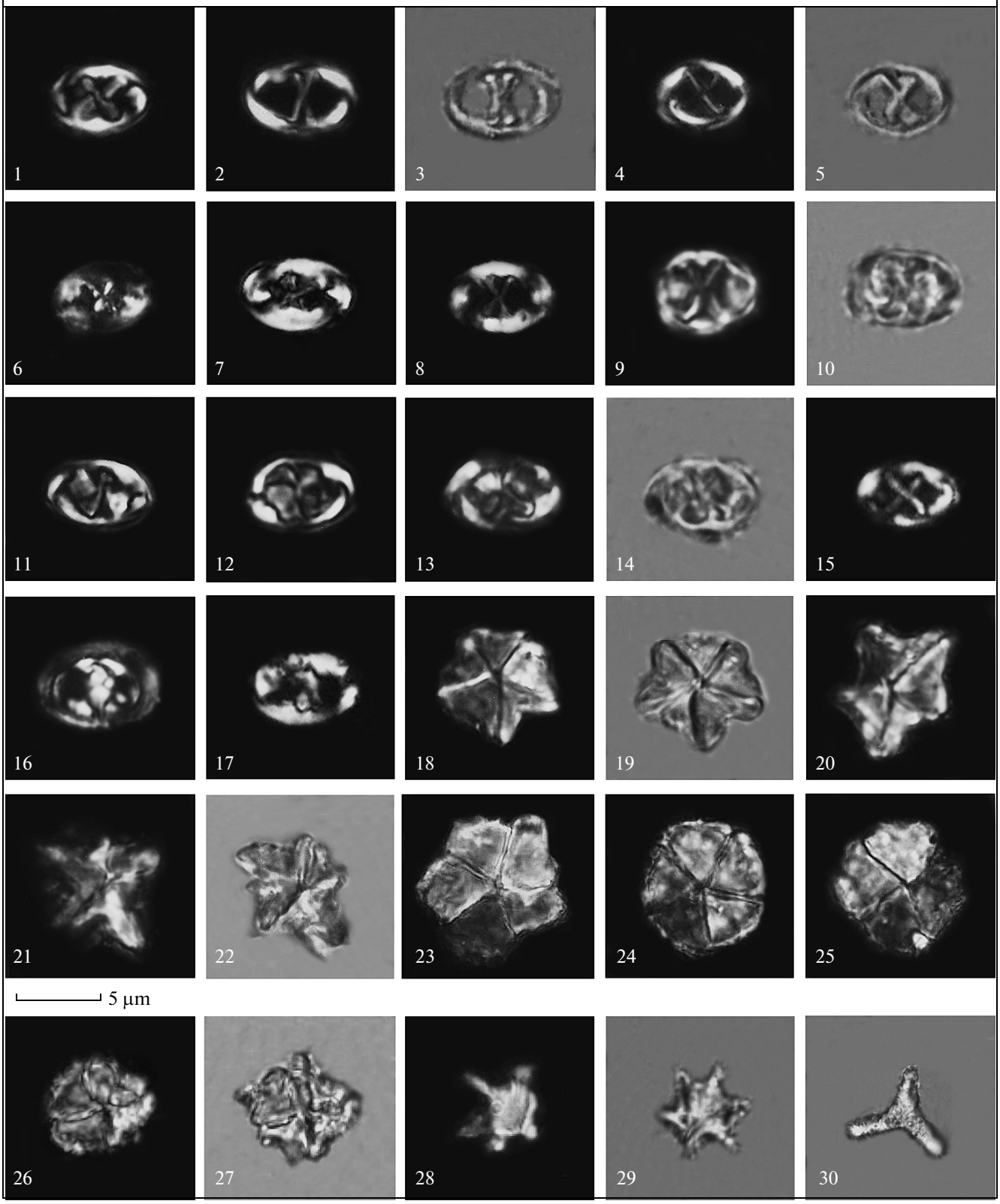
1
2
3
4
5
6
7
8
9
10
11
12
13
14
15
16
17
18
19
20
21
22
23
24
25
5 μm
26
27
28
29
30

In the interval of NP6–NP7 zones, the local Alisocysta margarita zone was recognized. Noteworthy, the interval of the stratigraphic range of this species in the NW Europe dinocyst zonation is partly restricted to the D4a–D4b subzones and can be correlated to the terminal part of the NP5 and NP7 zones (Luterbacher et al., 2004). In the Danian Basin, this taxon appears at the base of the Viborg 3 zone (Heilmann-Clausen, 1985, 1994) and can be correlated with the top of the NP5 zone. Thus, *Alisocysta margarita* occurs later within the studied area.

A rapid diversification of the nannofossils started in the Thanetian involving mainly genera *Neochiastozygus* and *Chiasmolithus* and in the later stage—*Fasciculithus* and *Discoaster*. Comparing to nannofossil assemblagesof more western regions of the Caucasus and Eastern Crimea, the Thanetian nannofossils of the Urma Plateau are characterized by relatively smaller size and low diversity of heliolits, represented by three species only, but higher diversity of Toweius. Dinocysts occur only in the lower and upper parts of the Thanetian. Both dinocyst and planktonic foraminifer assemblages are characterized by low diversity that does not allow estimation of turnover rate. The 3rd radiation of fasciculiths began in the upper part of the NP8 zone with the FO of *F. lillianae*, followed by FOs of enormously large *F. schaubii*, *F. richardii*, *F. thomasii*, *F. allanii*, and *F. sidereus* in the NP9 zone. Interesting is early occurrence of large chiasmoliths (*C. eograndis* and *C. californicus*) in the NP8 zone, which usually appear later in the Crimea–Caucasus region (near the base of the NP9 zone). The FO of *Morozovella aequa* coincides with FO of *Discoaster multiradiatus* that defines possible correlation of the lower boundaries of the NP9 and Acarinina acarinata zones. Dinocysts re-appear again in the middle of the NP9 zone. The dinocyst assemblage includes several species of the genus *Apectodinium* that is typical for dinocyst assemblages in different parts of the world (Powell, 1992; Heilmann-Clausen, 1994; Luterbacher et al., 2004).

As was mentioned above, the Paleocene/Eocene transition is characterized by complex combination of weak erosion and substantial submarine slumping. It is important to note the evidence of primary accumulation of sediments rich in TOC in the earliest Eocene of Ostrich Farm section similarly to some other Paleogene sections of Dagestan (Chirkey, Verkhnii Dzhengutay, and Gubden) (Gavrilov et al., 2003; Gavrilov and Shcherbinina, 2009) and occurrence of rhomboasters and asymmetric discoasters (*D. anartios*) nannofossils corresponding to the PETM event. In all likelihood, sedimentation in this interval was primary continuous, because short-lived species *Tribrachiatus digitalis* ranging NP10c subzone occurs in the assemblage with "excursion taxa" corresponding to PETM and later superimposed processes disturbed normal bedding. Besides, the Thanetian/Ypresian transition is characterized by the FOs of *Wetzeliella astra* and *W. lobisca* (the upper part of the NP10 zone).

The early Eocene nannofossils show the normal succession of FOs and the speciality of the assemblage is the occurrence of abundant *Zygrhablithus bijugatus* and *Toweius callosus* and common sphenoliths and rabdosphaerides. This likely indicates the sedimentation in shallow environment. The interval of the NP10–NP12 zones is characterized by successive FOs of dinocysts: *Biconidinium longissimum*, *Deflandrea phosphoritica*, *Dracodinium simile*, *Rhombodinium translucidum*, *Wetzeliella uncinata*, *Diphyes ficusoides*, *Dracodinium varielongitudum*, *Wetzeliella unicaudalis*, *Wilsonidium tabulatum*, *Dracodinium politum*, and *Cerebrocysta bartonensis*. Within the NP11 zone, a short stratigraphic hiatus, corresponding to the Wetzeliella meckelfeldensis zone, is revealed.

The middle Eocene nannofossil assemblage is very poor, but species diversity is still sufficient for zonal subdivision of deposits. It must be stipulated that some outcrops of the upper part of this sequence (Fig. 5) are located at considerable distance between them. Despite the fact that these outcrops belong to the same stratigraphic range, there is no absolute cer-

Plate V. Light microscope images of nannofossils of the Ostrich Farm section. (1) *Neochiastozygus chiastus* (Bramlette et Sullivan) Perch-Nielsen, sample 145, PL; (2) *Neochiastozygus perfectus* Perch-Nielsen, sample 149, PL; (3) the same specimen, OL; (4) *Neochiastozygus concinnus* (Martini) Perch-Nielsen, sample 149, PL; (5) the same specimen, OL; (6) *Neochiastozygus distentus* (Bramlette et Sullivan) Perch-Nielsen, sample 151, PL; (7) *Neochiastozygus distentus* (Bramlette et Sullivan) Perch-Nielsen, sample 119, PL; (8) *N. distentus*, sample 124, PL; (9) *N. denticulatus*, sample 151, PL; (10) the same specimen, OL; (11) *Neochiastozygus* sp. 1, sample 151, PL; (12) *Neochiastozygus* sp. 1, sample 151, the same sample, OL; (13) *Neochiastozygus* sp. 1, sample 143, PL; (14) the same specimen, OL; (15) *Neochiastozygus digitosus* Perch-Nielsen, sample 164, PL; (16) *Placozygus sigmoides* Bramlette et Sullivan, sample 144, PL; (17) *Zygodiscus* sp., sample 165, PL; (18) *Micrantolithus entaster* Bramlette et Sullivan, sample 142, PL; (19) the same specimen, OL; (20) *Micrantolithus pinguis* Perch-Nielsen, sample 141, PL; (21) *Micrantolithus* sp., sample 141, PL; (22) the same specimen, OL; (23) asymmetrical specimen of *Braarudosphaera bigelowii* (Gran et Braarud) Deflandre, sample 145, PL; (24) *Braarudosphaera discula* Bramlette et Riedel, sample 144, PL; (25) *Braarudosphaera?* sp., sample 8-1, PL; (26) *Nannotetrina?* sp.?, sample 131, PL; (27) the same specimen, OL; (28) *Rhomboaster bramlettei* (Bronniman et Stradner) Bybell et Self-Trail, sample 124, PL; (29) *Rhomboaster cuspis* Bramlette et Sullivan, sample 126-3, PL; (30) *Tribrachiatus orthostylus* Shamrai, sample 8-5, OL.

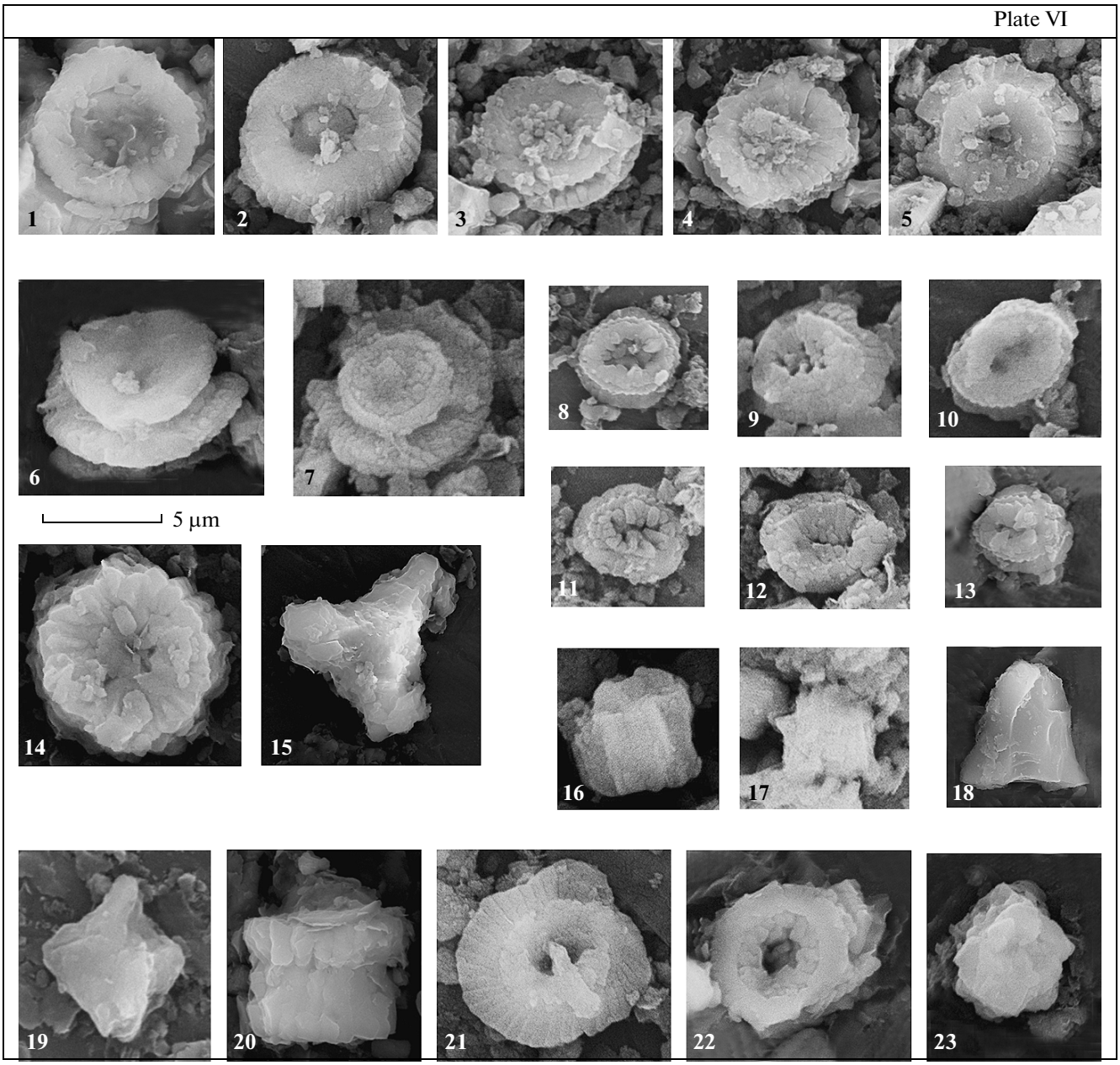

Plate VI. SEM images of nannofossils of the Ostrich Farm section. (1) *Coccolithus robustus* (Bramlette et Sullivan) Wind et Wise, sample 145; (2) *Coccolithus subpertusus* (Hay et Mohler) Wei et Pospichal, sample 145; (3) *Coccolithus* sp. 1, sample 145; (4) *Coccolithus* sp. 1, another sample, sample 145; (5) *Coccolithus* sp. 2, sample 145; (6) *Coccolithus subpertusus*, sample 152; (7) *Heliolithus?* sp. 1, sample 170; (8) *Toweius pertusus* (Sullivan) Romein, distal view, sample 145; (9) *Toweius pertusus* (Sullivan) Romein, proximal view, sample 152; (10) *Prinsius martini* (Perch-Nielsen) Haq, sample 152; (11) *Prinsius dimorphosus* Perch-Nielsen, sample 145; (12) *Prinsius bisulcus* (Stradner) Hay et Mohler, sample 152; (13) *Prinsius tenuiculus* (Okada et Thierstein) Varol et Jakubowski, sample 145; (14) *Heliolithus aktasii* Varol, sample 116; (15) *Tribrachiatus orthostylys* Shamrai, sample 126-3; (16) *Lithoptychius billii* (Perch-Nielsen) Aubry, sample 145; (17) *Lithoptychius varolii* (Steurbaut et Sztrakos) Aubry, sample 145; (18) *Fasciculithus clinatus* Bukry, sample 116; (19) *Rhomboaster cuspis* Bramlette et Sullivan, sample 126-3; (20) *Lythoptychius* sp. 2 sensu Aubry et al. (2011), sample 116; (21) *Helicosphaera?* sp., sample 170; (22) unknown nannofossil, sample 116; (23) *Lithoptychius* sp., sample 145.

Plate VII. Light microscope images of dinocysts of the Ostrich Farm section. (1) *Alisocysta* sp. 2 Heilmann-Clausen, 1985; (2) *Operculodinium centrocarpum* (Deflandre et Cookson) Wall; (3, 4, 11) *Achomosphaera alcicornu* (Eisenack) Davey et Williams; (5) *Deflandrea oebisfeldensis* Alberti; (6) *Adnatosphaeridium* sp. 1; (7) *Wilsonidium pechoricum* Iakovleva et Heilmann-Clausen; (8) *Danea* sp. 1; (9) *Heslertonia heslertonensis* Neale et Sarjeant; (10) *Apectodinium augustum* (Harland) Lentin et Williams; (11) *Spiniferites septatus* Cookson et Eisenack; (12) *Spiniferites* sp.; (13) *Apectodinium homomorphum* (Deflandre et Cookson) Lentin et Williams; (14) *Wilsonidium tabulatum* (Wilson) Lentin et Williams.

Plate VII

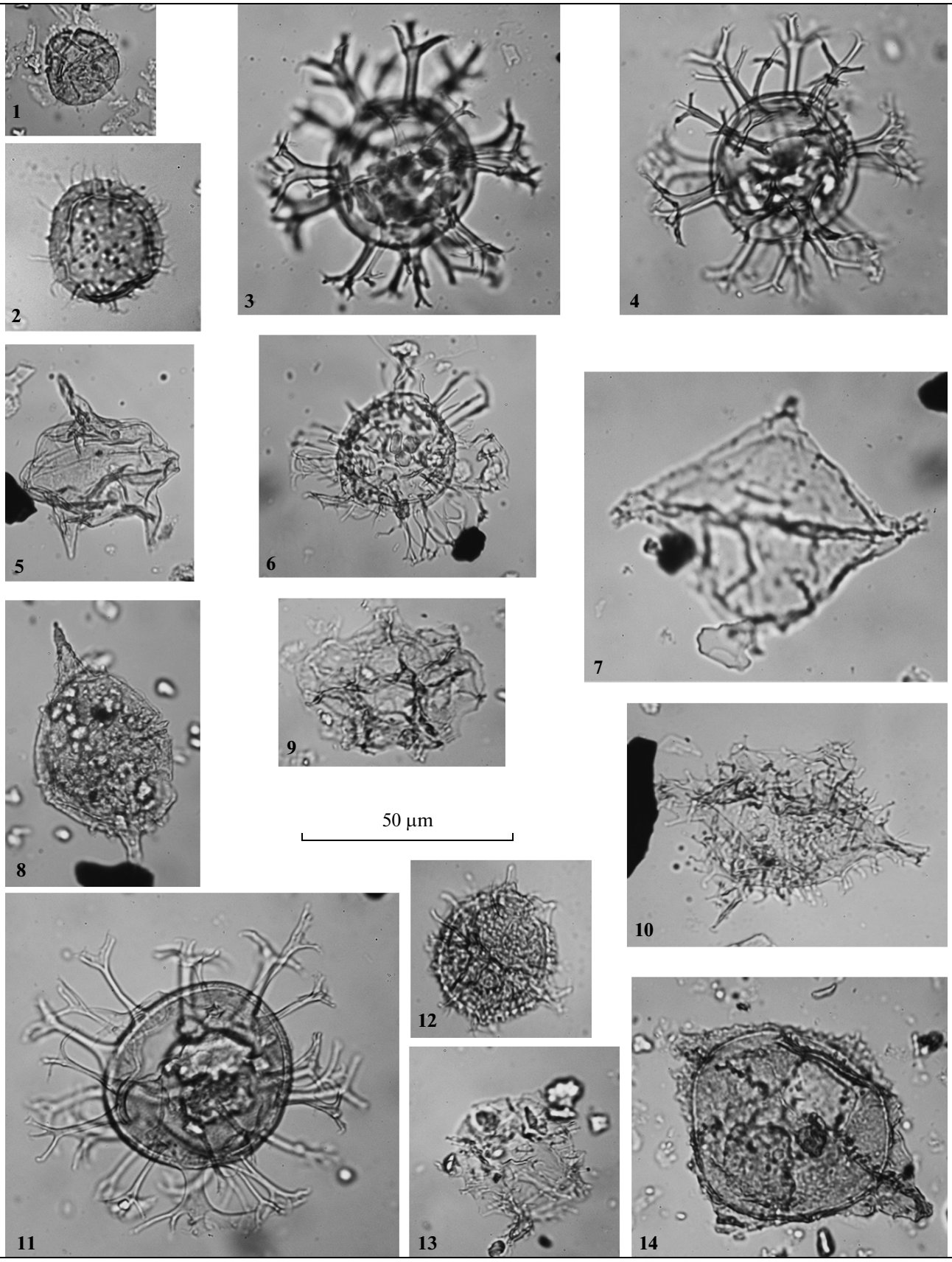

Plate VIII

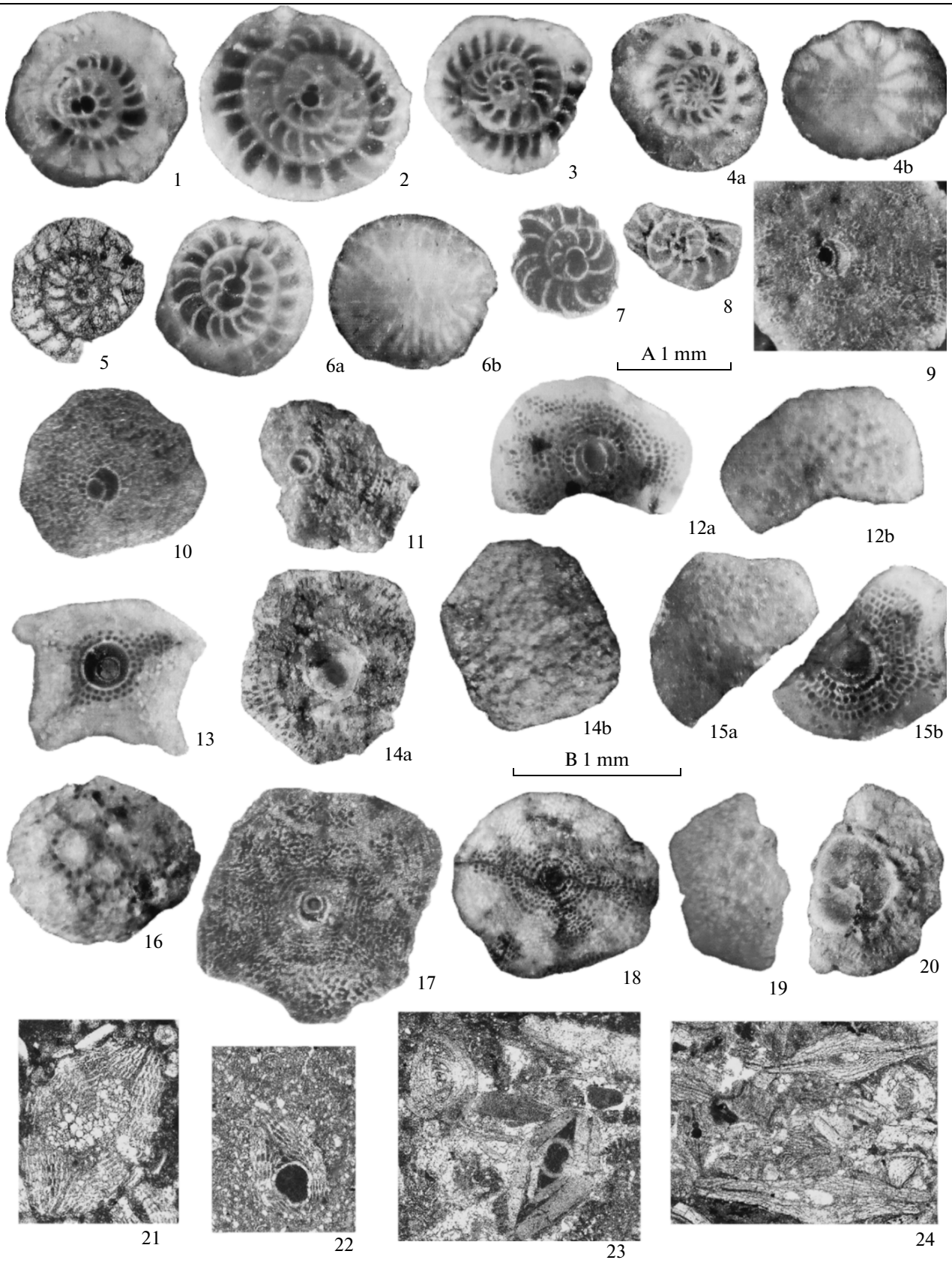
1
2
3
4a
4b
5
6a
6b
7
8
A 1 mm
9
10
11
12a
12b
13
14a
14b
15a
15b
B 1 mm
16
17
18
19
20
21
22
23
24

Plate VIII. Light microscope images of the large foraminifers of Ostrich Farm section.
Magnification: figs. 1–8, 23, 24 (bar A), ×20; figs. 9–22 (bar B), ×30. (1–3, 5) *Nummulites soerenbergensis* Schaub, 1951, generation A, sample 8/5, equatorial sections; (4) *Nummulites* cf. *praelucasi* Douville, 1924, generation B, sample 8/5, equatorial section and surface; (6, 7) *Nummulites* cf. *increscens* Schaub, 1951, generation A, sample 8/5: (6) equatorial section and surface, (7) equatorial section; (8) *Operculina karreri* Penecke, 1885, generation A, sample 8/5, equatorial section; (9–12) *Orbitoclypeus douvillei yesilyurtensis* Özcan, 2002, generation A, sample 8/5: (9–12a) equatorial sections, (12b) surface; (13–15) *Orbitoclypeus schopeni crimensis* Less, 1987, generation A, sample 8/5: (13, 14a, 15b) equatorial sections; (14b, 15a) surfaces; (16–19) *Orbitoclypeus varians portnayae* Less, 1987, generation A, sample 8/5: (16, 19) surfaces, (17, 18) equatorial sections; (20) *Discocyclina archiaci* cf. *archiaci* (Schlumberger, 1903), generation A, sample 8/5, equatorial section; (21–24) axial sections of large foraminifers in thin sections of organogenic limestones: (21) *Orbitoclypeus schopeni* (Checcia-Rispoli, 1908) ssp. indet, generation A, sample 128; (22) *Orbitoclypeus douvillei* (Schlumberger, 1903) ssp. indet, generation A, sample 127-1-06; (23) *Nummulites* ex gr. *leupoldi* Schaub, 1951 (right bottom), generation A, large rotaliid (left top), sample k3; (24) two shells of *Discocyclina* cf. *dispansa* (Sowerby, 1840), generation A, sample 133-2.

tainty that we suggested the true stratigraphic correlation of this isolated exposures, especially, taking into account the high lateral variability of facies in this stratigraphic interval. Accordingly, it is difficult to estimate now the true thickness of Lutetian deposits of the Urma Plateau.

CONCLUSIONS

The co-occurrence of diverse assemblages of three groups of microplankton (nannofossils, foraminifera, and dinocysts) in the Ostrich Farm section provided the definition of the stratigraphic range of the studied deposits (upper Danian–Lutetian) and directly correlate the zones of the nannofossil standard zonation, the Crimea–Caucasus planktonic foraminifera scale, and the dinocyst scale. These permit to obtain valuable information for future correlation of Paleogene marine calcareous and non-calcareous deposits. Three hiatuses have been recognized in the section studied: at the Danian/Zelandian boundary (nannofossil subzones NTp8B–NTp8C), at the Paleocene–Eocene boundary (the NP9B subzone and the lower part of the NP10 zone), and in lower Eocene (dinocyst zone Wetzeliella meckelfeldensis). It is impossible to determine the duration of the hiatus preceding the accumulation of siliceous sequence, since microfossils are absent in its lower part and the stratigraphic range of missing intervals varies considerably laterally. The nannofossil study of the Gray Formation of the Urma Plateau confirmed with certainty that it is coeval to studied recently red Paleogene deposits of the northern regions of Dagestan (e.g., the section in the vicinity of Chirkey HPP) (Shcherbinina and Gavrilov, 2012).

Reviewers: M.A. Akhmetiev and E.M. Bugrova

ACKNOWLEDGMENTS

We thank Dr. Yu.O. Gavrilov for organization and leadership of the field works, careful reading of our manuscript, and advice concerning the lithological description of the studied deposits. We thank also Dr. E.M. Bugrova for constructive review of our manuscript, which helped to improve the paper. We appreciate the assistance of N.V. Gorkova in photographing the nannofossils under the SEM.

This work was supported by Russian Foundation for Basic Research, project no. 12-05-01138 and the Program NSh-4185.2008.5.

REFERENCES

Akhmetiev, M.A. and Beniamovskii, V.N., The Paleocene and Eocene in the Russian part of West Eurasia, *Stratigr. Geol. Correlation*, 2006, vol. 14, no. 1, pp. 54–78.

Aleksandrova, G.N. and Shcherbinina, E.A., Stratigraphy and paleoenvironmental interpretation of the Paleocene–Eocene transition in the Eastern Crimea, *Stratigr. Geol. Correlation*, 2011, vol. 19, no. 4, pp. 424–449.

Amon, E.O., Vasilyeva, O.N., and Zhelezko, V.I., Stratigraphy of the Talitsa Horizon (Paleocene) in the Central Trans-Urals, *Stratigr. Geol. Correlation*, 2003, vol. 11, no. 3, pp. 75–90.

Atlas of Paleocene planktonic foraminifera, *Smithsonian Contrib. Paleobiol.*, Olsson, R.K., Hemleben, C., Berggren, W.A., and Huber, B.T., Eds., 1999, no. 85.

Aubry, M.-P., Bord, D., and Rodrigez, O., New taxa of the Order *Discoasterales* Hay, 1977, *Micropaleontol.*, 2011, vol. 57, no. 3, pp. 269–287.

Aubry, M.-P., Ouda, K., Dupuis, C., et al., The global standard stratotype section and point (GSSP) for the base of the Eocene series in the Dababiya section (Egypt), *Episodes*, 2007, vol. 30, no. 4, pp. 271–286.

Aubry, M.-P., Rodrigez, O., Bord, D., Godfrey, L., Schmitz, B., and Knox, R., The first radiation of the fasciculiths: morphologic adaptations of the coccolithophores to oligotrophy, *Austrian J. Earth Sci.*, 2012, vol. 105, no. 1, pp. 29–38.

Beniamovskii, V.N., Detailed stratigraphic scheme for the Lower Paleogene of the Crimea–Caucasus region, in *Puti detalizatsii stratigraficheskikh skhem i paleogeograficheskikh rekonstruktsii* (Ways for Specification of Stratigraphic Scales and Paleogeographic Reconstructions), Moscow: GEOS, 2001, pp. 210–223.

Berggren, W.A. and Aubert, J., Paleocene benthonic foraminiferal biostratigraphy, paleobiogeography and paleo-

ecology of Atlantic–Tethyan regions: Midway-type fauna, *Palaeogeogr. Palaeoclimat. Palaeoecol.*, 1975, vol. 18, no. 2, pp. 73–192.

Berggren, W.A. and Pearson, P.N., A revised tropical to subtropical Paleogene planktonic foraminiferal zonation, *J. Foraminiferal Res.*, 2005, vol. 35, no. 4, pp. 279–298.

Bernaola, G., Martin-Rubio, M., and Baceta, J.I., New high resolution calcareous nannofossil analysis across the Danian/Selandian transition at the Zumaia section: comparison with South Tethys and Danish sections, *Geol. Acta*, 2009, no. 7, pp. 79–92.

Bown, P.R., Calcareous nannofossil biostratigraphy, in *British Micropalaeontol. Soc. Publ. Ser.,* London: Chapman and Hall Ltd. Kluwer Academic Publisher, 1998.

Clemmensen, A. and Thomsen, E., Palaeoenvironmental changes across the Danian–Selandian boundary in the North Sea basin, *Palaeogeogr. Palaeoclimat. Palaeoecol.*, 2005, no. 219, pp. 351–394.

Crouch, E.M., Heilmann-Clausen, C., Brinkhuis, H., et al., Global dinoflagellate event associated with the Late Paleocene thermal maximum, *Geology*, 2001, vol. 29, pp. 315–318.

Crouch, E.M., Brinkhuis, H., Vissher, H., et al., Late Paleocene–Early Eocene dinoflagellate cyst records from the Tethys: further observations on the global distribution of *Apectodinium*, in *Causes and Consequences of Globally Warm Climates in the Early Paleogene*, Wing, S.L., Gingerich, P.D., Schmitz, B., and Thomas, E., Eds., *Geol. Soc. Am. Spec. Pap.*, 2003, no. 369, pp. 113–131.

Galin, V.L., Akaev, B.A., and Smirnov, Yu.P., Some data about stratigraphy and lithofacies of the foraminiferal formation of the piedmont zone of Dagestan, in *Voprosy geologii i neftegazonosnosti paleogena Predgornogo Dagestana* (Problems of Geology and Oil and Gas Potential of the Paleogene Deposits of the Piedmont Zone of Dagestan), Musaev, S.E., Ed., *Tr. Inst. Geol. Dagestan Filial AN SSSR*, 1963, Iss. IV, pp. 3–10.

Gavrilov, Yu.O., Shcherbinina, E.A., and Oberhänsli, H., Paleocene/Eocene boundary events in the northeastern Peri-Tethys, in *Causes and Consequences of Globally Warm Climates in the Early Paleogene*, Wing, S.L., Gingerich, P.D., Schmitz, B., and Thomas, E., Eds., *Geol. Soc. Am. Spec. Pap.*, 2003, no. 369, pp. 147–168.

Gavrilov, Yu.O. and Shcherbinina, E.A., A variety of PETM effects in different settings of northeastern Peri-Tethys, in *Extend. Abstr. Int. Conf. "Climatic and Biotic Events of the Paleogene (CBEP)," January 12–15, 2009, Wellington, New Zealand*, Strong, P.C., Crouch, E.M., and Hollis, C., Eds., *GNS Miscellaneous*, 2009, no. 16, pp. 67–70.

Golubyatnikov, V.D., About intraformational dislocations at the Cretaceous–Tertiary boundary in the deposits of Dagestan, *Mat. Tsentr. Nauchno-Issled. Geol.-Razved. Inst., Obshch. Ser.*, 1938, Iss. 3, pp. 23–49.

Golubyatnikov, V.D., *Geologiya i poleznye iskopaemye tretichnykh otlozhenii Dagestana* (Geology and Mineral Recourses of Tertiary Deposits of Dagestan), L.–M.: Gosgeolizdat, 1940.

Heilmann-Clausen, C., Dinoflagellate stratigraphy of the uppermost Danian to Ipresian in the Viborg 1 borehole, Central Jylland, Denmark, *Danmarks Geologiske Undersogelse*, *Ser. A*, 1985, no. 7, pp. 1–69.

Heilmann-Clausen, C., Review of Paleocene dinoflagellates from the North Sea region, in *Proc. Meet. "Stratigraphy of the Paleocene," GFF*, 1994, vol. 116, pp. 51–53.

Luterbacher, H.P., Ali, J.R., Brinkhuis, H., et al., The Paleogene period, in *A Geologic Time Scale 2004*, Gradstein, F.M., et al., Eds., Cambridge: Univ. Press, 2004, pp. 384–408.

Martini, E., Standard Tertiary and Quaternary calcareous nannoplankton zonation, in *Proc. 2nd Planktonic Conf., Rome, 1970*, Farinacci, A., Ed., *Edizioni Tecnoschienza*, 1971, no. 2, pp. 739–785.

Mikulenko, K.I., On stratigraphic relationships between Variegated and Gray Formations of lower Paleogene in Dagestan, *Dokl. Akad. Nauk SSSR*, 1962, vol. 142, no. 1, pp. 171–172.

Mudge, D.C. and Bujak, J.P., An integrated stratigraphy for the Paleocene and Eocene of the North Sea, *Geol. Soc. Spec. Pap. London,* 1996, vol. 101, pp. 91–113.

Muzylev, N.G., *Stratigrafiya paleogena Yuga SSSR po nannoplanktonu (Severnyi Kavkaz i Krym)* (The Paleogene Nannoplankton Stratigraphy of the Southern USSR (Northern Caucasus and Crimea)), Moscow: Nauka, 1981 [in Russian].

Okada, H. and Bukry, D., Supplementary modification and introduction of code numbers of the low-latitude coccolith biostratigraphic zonation (Bukry 1973, 1975), *Mar. Micropalaeontol.*, 1980, vol. 5, pp. 321–325.

Perch-Nielsen, K., Cenozoic nannofossils, in *Plankton Stratigraphy*, Bolli, H.M., Saunders, J.B., and Perch-Nielsen, K., Eds., Cambridge: University Press, 1985, pp. 427–554.

Powell, A.J., Dinoflagellate cysts of the Tertiary System, in *A Stratigraphic Index of Dinoflagellate Cysts*, Powell, A.J., Ed., *British Micropaleontol. Soc. Publ. Ser.*, London: Chapman and Hall, 1992, pp. 151–251.

Prakticheskoe rukovodstvo po mikrofaune. T. 8. Foraminifery kainozoya (Practical Manual on Microfauna of the USSR. Vol. 8: Cenozoic Foraminifers), St. Petersburg: Izd. VSEGEI, 2005 [in Russian].

Schmitz, B., Pujalte, V., Molina, E., et al., The global stratotype sections and points for the bases of the Selandian (Middle Paleocene) and Thanetian (Upper Paleocene) stages at Zumaia, Spain, *Episodes*, 2011, vol. 34, no. 4, pp. 220–243.

Shatskii, N.S., Geological Structure of the Eastern Part of the Black Mountains and the Miatly and Dylym Oil Fields (Northern Dagestan), in *Shatskii N.S. Izbrannye trudy. T. 1* (Shatskii N.S. Selected Papers. Vol. 1), Moscow: Izd. AN SSSR, 1963, pp. 115–216.

Shcherbinina, E.A. and Gavrilov, Yu.O., Stratigraphy of Cretaceous and Lower Paleogene sediments in central Dagestan based on nanoplankton, in *Regional Geology and Oil-and-Gas Potential of the Caucasian Region*, Cherkashin, V.I., Ed., 2012, pp. 57–65.

Shutskaya, E.K. and Kuznetsova, K.I., Correlation of Variegated and Gray Formations of Dagestan, *Byull. Mosk. O-va Ispyt. Prir., Otd. Geol.,* 1953, vol. 28, no. 6, pp. 75–78.

Shutskaya, E.K., *Stratigrafiya, foraminifery i paleogeografiya nizhnego paleogena Kryma, Predkavkaz'ya i zapadnoi chasti Srednei Azii* (Stratigraphy, Foraminifers, and Paleogeography of the Lower Paleogene in the Crimea, Ciscaucasus, and Western Part of Central Asia), Moscow: Nedra, 1970 [in Russian].

Sprong, J., Speijer, R.P., and Steurbaut, E., Biostratigraphy of the Danian/Selandian transition in the southern Tethys. Special reference to the lowest occurrence of planktic foraminifera *Igorina albeari*, *Geol. Acta,* 2009, no. 7, pp. 63–77.

Steurbaut, E. and Sztrakos, K., Danian/Selandian boundary criteria and North Sea basin–Tethys correlations based on calcareous nannofossil and foraminiferal trends in SW France, *Mar. Micropalaeontol.*, 2008, no. 67, pp. 1–29.

Thomsen, E. and Heilmann-Clausen, C., The Danian–Selandian boundary sequence at Svejstrup and remarks on the biostratigraphy of the boundary in Western Denmark, *Bull. Geol. Soc. Denmark*, 1984, no. 33, pp. 339–360.

Varol, O., Palaeocene calcareous nannofossil biostratigraphy, in *Nannofossils and Their Applications*, Crux, J.A. and van Heck S.E., Eds., *British Micropalaeontol. Soc.*, 1989, no. 12, pp. 267–310.

Vasilyeva, O.N., Stratigraphy of Paleocene Deposits in the Loz'va River Basin (Northern Urals) based on palynological data, in *Problemy stratigrafii i paleontologii Urala* (Problems in Stratigraphy and Paleontology of the Urals), Yekaterinburg: IGG UrO RAN, 1999, pp. 170–175.

Vasilyeva, O.N., On the correlation of Danian/Selandian boundary deposits of Caspian Sea region and Western Siberia, *Ezhegodnik–2009. Tr. IGG UrO RAN*, 2010, Iss. 157, pp. 11–16.

Vasilyeva, O.N. and Musatov, V.A., Biostratigraphic subdivision of the Paleogene sequence of the Novy Uzen' stratigraphic test well based on dinocysts and nannofossils: preliminary results, *News on Paleontology and Stratigraphy.* Iss. 10–11. *Suppl. Geol. Geofiz.*, 2008, vol. 49, pp. 347–350.

Youssef Ali, M., High resolution calcareous nannofossil biostratigraphy and paleoecology across the latest Danian event (LDE) in Central Eastern Desert, Egypt, *Mar. Micropalaeontol.*, 2009, no. 72, pp. 111–128.

Translated by D. Voroschuk